

REPORT DOCUMENTATION PAGE		READ INSTRUCTIONS BEFORE COMPLETING FORM
1. REPORT NUMBER 18	2. GOVT ACCESSION NO.	3. RECIPIENT'S CATALOG NUMBER
4. TITLE (and Subtitle) Signal Detection and Normalization in Underwater Noises Modeled as a Gaussian-Gaussian Mixture		5. TYPE OF REPORT & PERIOD COVERED Technical Report Sept. 1984-August 1985
7. AUTHOR(s) Michel Bouvet and Stuart C. Schwartz		6. PERFORMING ORG. REPORT NUMBER
9. PERFORMING ORGANIZATION NAME AND ADDRESS Information Sciences & Systems Laboratory Dept. of Electrical Eng. & Computer Sci. Princeton University, Princeton, NJ 08544		8. CONTRACT OR GRANT NUMBER(s) N00014-81-K-0146
11. CONTROLLING OFFICE NAME AND ADDRESS Office of Naval Research (Code 411SP) Department of the Navy Arlington, Virginia 22217		10. PROGRAM ELEMENT, PROJECT, TASK AREA & WORK UNIT NUMBERS NR SRO-103
14. MONITORING AGENCY NAME & ADDRESS (if different from Controlling Office)		12. REPORT DATE January 1986
		13. NUMBER OF PAGES 58
		15. SECURITY CLASS. (of this report) Unclassified
		15a. DECLASSIFICATION/DOWNGRADING SCHEDULE
16. DISTRIBUTION STATEMENT (of this Report) Approved for public release; distribution unlimited		
17. DISTRIBUTION STATEMENT (of the abstract entered in Block 20, if different from Report)		
18. SUPPLEMENTARY NOTES A portion of this report has been submitted to the Journal of the Acoustical Society of America and another portion to ICASSP '86.		
19. KEY WORDS (Continue on reverse side if necessary and identify by block number) underwater noise models Gaussian-Gaussian mixture power normalization robust and adaptive detection		
20. ABSTRACT (Continue on reverse side if necessary and identify by block number) Knowledge of the noise probability density function (PDF) is central in signal detection problems, not only for optimum receiver structures but also for processing procedures such as power nor- malization. Unfortunately, the statistical knowledge must be ac- quired since the classical assumption of a Gaussian noise PDF is often not valid in underwater acoustics. In this report, we study statistical modeling by a Gaussian-Gaussian mixture for three different underwater noise samples. We show that one of them can Cont.		

REPORT NUMBER 18.

SIGNAL DETECTION AND NORMALIZATION IN UNDERWATER NOISES MODELED AS A GAUSSIAN-GAUSSIAN MIXTURE

M. BOUVET and S.C. SCHWARTZ

INFORMATION SCIENCES AND SYSTEMS LABORATORY.

Department of Electrical Engineering
Princeton University.
Princeton, New Jersey 08544

JANUARY 1986

Prepared for

OFFICE OF NAVAL RESEARCH (Code 411SP)
Statistics and Probability Branch
Arlington, Virginia 22217
under Contract N00014-81-K0146
Program in Ocean Surveillance and Signal Processing
S.C. Schwartz, Principal Investigator

Approved for public release; distribution unlimited

SIGNAL DETECTION AND NORMALIZATION
IN UNDERWATER NOISES MODELED AS A GAUSSIAN-GAUSSIAN MIXTURE

*Michel BOUVET** and *Stuart C. SCHWARTZ*

Department of Electrical Engineering
Princeton University
PRINCETON, NJ 08544

ABSTRACT

Knowledge of the noise probability density function (PDF) is central in signal detection problems, not only for optimum receiver structures but also for processing procedures such as power normalization. Unfortunately, the statistical knowledge must be acquired since the classical assumption of a Gaussian noise PDF is often not valid in underwater acoustics. In this report, we study statistical modeling by a Gaussian-Gaussian mixture for three different underwater noise samples. We show that one of them can adequately be described by a Gaussian-Gaussian mixture, one is very close to a Gaussian model and is described by a mixture with a very small perturbing term, whereas the third one seems closer to the Middleton class A model but is non-stationary.

* On leave from Groupe d'Etude et de Recherche en Detection Sous-Marine, Le Brusac, 83140 SIX-FOURS LES PLAGES (FRANCE).

Key-words: non-Gaussian detection, adaptive normalization, noise model, underwater noises.

The first noise is studied with emphasis on the normalization needed in the receiver in order to achieve a constant false alarm probability and also on the optimal receiver structure for the detection of a deterministic signal. It is shown that the classical noise power estimate, calculating the norm L^2 of the observation vector, is a good approximation to the square of the maximum likelihood estimator of the noise amplitude for the Gaussian-Gaussian mixture. The notion of noise alone reference is investigated and the performances of normalized test-functions using different power estimates are studied. Finally, a comparison is made between the *adaptive* mixture likelihood ratio and the *robust* matched filter and soft-limiter. The principal result is that the use of the receiver associated with the mixture model leads to improvements with respect to these two classical receivers, this improvement being measured in terms of receiver operating characteristics (ROC) curves.

At low false alarm rates (10^{-4}) and SNR levels around -5 dB, this improvement can be especially significant; one situation shows an improvement in detection probability from 0.4 to 0.6, a 50 % increase.

1. INTRODUCTION

The Bayesian theory of detection of a known deterministic signal in additive noise is based on the knowledge of the noise probability density function (PDF) [1,2]. The normalized noise PDF is important for the receiver structure and the amplitude of the noise (scale) allows power normalization [3]. Unfortunately, the classical assumption of a Gaussian PDF is often not valid in real-world problems such as those encountered in sonar applications [4,5,6]. A variety of other PDFs have been proposed to fit real data. Among these models, two in particular appear to describe underwater acoustical noises: the Middleton class-A model and the Gaussian-Gaussian mixture [4,7,8]. The Middleton model is physically motivated but has the disadvantage of having a PDF represented by an infinite expansion of Gaussian PDFs. However, Vastola has shown that for many interesting cases, only the first two terms of this expansion are sufficient from a detection point of view [9], in which case we can work with a Gaussian-Gaussian mixture model. This report is “engineering oriented”, and can be viewed as a preliminary investigation of the possible improvement of the likelihood receiver when the noise is modeled by a Gaussian-Gaussian mixture instead of a Gaussian PDF.

In particular, we study three different underwater acoustic noises. We show that one, mostly generated by biological phenomenon, appears to be non-stationary, whereas one can be considered as almost Gaussian. The last noise is studied with emphasis on the normalization needed in the receiver in order to achieve a constant false alarm probability. It is shown that the classical noise power estimate, calculating the norm L^2 of the observation vector, is a good approximation of the square of the maximum likelihood estimator of the noise amplitude for a Gaussian-Gaussian mixture, under the assumption that the perturbing noise of the mixture is a small one.

Then, the notion of noise alone reference (NAR) is investigated. Basically, the estimate of the noise power must not be influenced by the possible presence of a signal. We compare, on the basis of receiver operating characteristics (ROC) curves, four normalized test-functions whose structure is either a matched filter, equivalent to the likelihood ratio for the Gaussian assumption, or the likelihood ratio associated with the mixture model. Each one is constructed using a particular noise amplitude estimate. This estimate could be a NAR or not, and is calculated under an assumption of a Gaussian or a Gaussian-Gaussian mixture PDF. Finally, a comparison is made between the *adaptive* mixture likelihood ratio receiver and the *robust* matched filter and soft-limiter.

2. THE DATA

2.1. Data Collection

The data studied here are typical underwater acoustic noises. They have been recorded with a single omnidirectional hydrophone. Three sets have been processed. The first one, called MS in the sequel, has been generated mostly by merchant ships and has been recorded in the Indian Ocean. The second one, called SS, is principally due to biological phenomenon, mostly snapping shrimp. This set has been recorded in an area around Hawaii, in shallow water. The third one, called BG, is an ambient background noise, mostly wind generated and perhaps containing distant shipping and biological noises, without a principal noise source. This noise has also been collected in the Indian Ocean and has been previously studied in another context [10]. The MS and BG data have been sampled at a rate 1250 Hz, i.e. 0.8 ms separates two samples, whereas the SS data has been sampled at 40 kHz.

2.2. Preliminary Study

Before doing a more detailed statistical investigation of these noises, the study of some very rough statistics can be helpful. 1000 samples of the data have been used. The noises have been normalized to second-order, i.e., their empirical global means and variances on the whole window are respectively 0 and 1. Figures 2.1 to 2.9 show the data and their local means and variances for the MS, SS, BG noises, respectively. The means and the variances have been calculated based on 20 samples, using a sliding window.

MS noise and BG noise seem to be stationary in appearance. Their variances vary roughly between 0.5 and 2.5. SS noise exhibits either in its appearance or in the computation of its variance some non-stationarities, located around the samples 200, 390, 570 and 960, for this set. Its variance varies between 0.2 and 11.0. The scales for the representations of the observation (Fig. 2.4) and the variance (Fig. 2.6) are different for this noise than those for the other ones. Hence, this last noise seems to have impulsive components. Its variance (power) is neither quasi-stationary, as assumed in [3], nor impulsive, following [5] where the noise power was constrained to take only two values. The presence of these impulsive components or bursts has already been found in another kind of noise, generated by ice-cracking phenomenon under the Arctic [11].

3. NOISE PDF MODELS

Mixture noise models have been developed in order to generalize the form of the noise PDF to better fit the data. These models correspond to a noise PDF that is a sum of elementary PDFs, usually the sum of only two, the most important being Gaussian. Recent studies of these models have shown they described quite accurately real data, especially in underwater acoustics [4,6,9]. In all this work, the noises will be assumed white. The PDFs are then univariate.

3.1. Middleton Model

The Middleton class-A noise model can be represented by an infinite series of Gaussian density-like terms,

$$p(x) = \sum_{m=0}^{\infty} K_m g(x; \sigma_m), \quad (3.1)$$

where $g(x; \sigma)$ is a Gaussian PDF with variance σ^2 [7,8]. The coefficients K_m are related to the *overlap index* A by the following relation,

$$K_m = e^{-A} \frac{A^m}{m!}. \quad (3.2)$$

The variances σ_m^2 are related to A and to another parameter Γ , the *Gaussian factor*, by

$$\sigma_m^2 = \frac{\frac{m}{A} + \Gamma}{1 + \Gamma}. \quad (3.3)$$

This model is a physically motivated one, modeling an impulsive interference noise, i.e., a Gaussian noise with an additive impulsive noise component. The model appears to fit quite well a variety of noise situations. The class-A model assumes that the noise bandwidth is less than that of the receiver ⁽¹⁾ [6]. In addition, it is difficult to compute with, due to the infinite series (3.1).

3.2. Mixture Gaussian-Gaussian PDF

The noise has, in this case, a PDF composed of the sum of two individual Gaussian PDFs,

$$p(x) = (1-\epsilon)g(x; \sigma_1) + \epsilon g(x; \sigma_2). \quad (3.4)$$

The philosophy of this PDF is to fit noise that can be considered as nearly Gaussian.

(1) Another noise model, class B, is suitable for the broadband case [7].

The proximity to the Gaussian PDF is due to the term $(1-\epsilon)g(x;\sigma_1)$, where ϵ and $1-\sigma_1$ are assumed to be small. In addition, the departure from the Gaussian assumption is modeled by the term $\epsilon g(x;\sigma_2)$, where $\sigma_2 > 1 > \sigma_1$. In particular, this component can take into account a small amount of kurtosis and tails longer than that for the individual Gaussian density in order to model impulsive components [4]. It can also model a PDF with a kurtosis smaller than for the Gaussian PDF [12].

Two other models with a **Gaussian-Gaussian mixture** have been used. The first model is a “Gaussian-Gaussian switched burst noise”, where the PDF is represented as in (3.4) but where ϵ is considered as a Bernoulli random variable, taking the value 0 or 1 [5,14]. This second model is complicated to deal with because it needs an estimation of the switched time-instants for the construction of the ideal or “clairvoyant” receiver.

The second one is the spherically invariant noise [13]. The univariate PDF of the observation is taken as

$$p(x) = a g(x;1), \tag{3.5}$$

where a is a random process taking positive values. This second model seems more interesting and we are going to study in section 5 a closely related model, where the noise power will be considered as an unknown parameter. But, instead of using a Gaussian PDF as in (3.5), we will use a Gaussian-Gaussian mixture.

3.3. Middleton Model and Gaussian-Gaussian Mixture

The studies on the Middleton model have shown that, for real-world problems, the parameter A is often small, say between 0.001 and 0.3 [9]. Then, the first few coefficients K_m are rapidly decreasing, e.g., $K_2 = 0.016$ for $A = 0.2$. In particular, Vastola has shown that the truncation of the expansion (3.1), representing the class-A

model, to the first two terms, $m = 0$ and $m = 1$, often has little effect on the locally-optimal non-linearity of the receiver associated with this noise. This truncation leads to a Gaussian-Gaussian mixture,

$$q(x) = \alpha e^{-A} g\left(x; \frac{\Gamma}{1+\Gamma}\right) + \alpha A e^{-A} g\left(x; \frac{1/A + \Gamma}{1+\Gamma}\right), \quad (3.6)$$

where α is a parameter assuring that $q(x)$ is a PDF, $\alpha \triangleq \frac{e^A}{1+A}$.

Comparing (3.6) with the expression (3.4) of a Gaussian-Gaussian mixture, the two following relations must hold,

$$A = \frac{\epsilon}{1-\epsilon}, \quad (3.7)$$

$$\Gamma = \frac{\sigma_1^2}{1-\sigma_1^2}, \quad \text{if } \sigma_1^2 < 1. \quad (3.8)$$

Since

$$\sigma_2 = \frac{\frac{1}{A} + \Gamma}{1 + \Gamma}, \quad (3.9)$$

the interpretation of a Gaussian-Gaussian mixture as the truncation of a Middleton class-A model can be made only if the following relation holds between the parameters of the mixture,

$$\sigma_2^2 = \frac{1 - \epsilon - \sigma_1^2 + 2\sigma_1^2\epsilon}{\epsilon}. \quad (3.10)$$

4. STATISTICAL CHARACTERIZATION OF THE NOISES

4.1. Description

For each noise, a global observation window, 4000 samples, was divided into two smaller windows of 2000 samples each. The first one represents the beginning of the

recording and the second one, the end. For each of these three windows (4000, 2000 and 2000 samples), we computed some empirical statistical measures and some parameters associated with the two previously described mixture models. These statistical measures are the mean, the variance, the skewness and the kurtosis. As stated previously, the noises were normalized, zero-mean and unit-variance, in the global window.

The parameters of the class-A model were computed using a method of moments (MOM) introduced by Powell and Wilson [15]. The parameters of the Gaussian-Gaussian mixture were computed using two different methods. The first one is a method of moments (MOM), or more precisely an approximation of this method which is easier to implement. This method can be found in Appendix A. The second one is a least-square method which deals with the Moment Generating Function (MGF) [16] and is described in Appendix B.

4.2. Results

As all the noises have been normalized, it is clear that they are zero-mean and unit-variance on the whole observation window. In the following discussion, we refer to Tables I-III.

* *Merchant Ships*

The statistical parameters are almost the same in the three windows, indicating that this noise can be considered as stationary. The skewness is small but the kurtosis, around 2.2, is quite different than that associated with the Gaussian PDF, i.e., 3. This can be explained by the fact that this noise is generated by radiated lines coming from ships and that the kurtosis of a spectral line is 1.5 [12]. The computation for a Middleton model fails. The results for the Gaussian-Gaussian mixture parameters are close to what is expected, i.e., a small ϵ , σ_1 not far from 1 and $\sigma_2 > 1$. This is true for both methods.

Based on this preliminary study with simple statistics, it appears that the MS noise can be adequately described by a Gaussian-Gaussian mixture model.

* *Snapping Shrimp*

This noise is highly non-stationary as the values of the statistical parameters on the three columns are different, in particular the variance and the kurtosis. This fact has already been noted in subsection 2.2, and on Figure II. We remark as in [11], that apparently a small amount of contamination (*outliers*) can give a great variation in the statistical characteristics. We also note that a larger kurtosis is due either to tails bigger than normal or to a highly peaked PDF.

In Table II, we note that the fitting procedure by the MOM for the Gaussian-Gaussian mixture fails, but not the procedure for the Middleton model. The values given by the Wilson method are close to values of similar noise samples studied [3,6,7,15]. The MGF method leads to reasonable parameters.

It seems reasonable to say that the principal characteristic of the SS noise is its non stationarity.

* *Background noise*

The same conclusions as in the MS case can be made, i.e., stationarity and statistical values close to Gaussian. The principal difference is that the kurtosis is closer to the Gaussian value of 3 and the skewness is a bit more significant. A look at the parameters for the Gaussian-Gaussian model shows that this noise seems to be very close to Gaussian, even closer than the MS noise.

Hence, the BG noise is well described by a Gaussian-Gaussian mixture, very close to a Gaussian PDF.

* *Comments*

The failure in the Middleton class-A fitting for the MS and BG noises can be due either to an inappropriate model or to a bad computational method, as mentioned by Wilson [15]. However, the parameters obtained for the Gaussian-Gaussian model are consistent with expected values.

4.3. Quantiles

For each noise, we have computed the quantiles with respect to the Gaussian PDF and to the Gaussian-Gaussian mixture. They are represented on Figures 4.1-4.3, each one corresponding to 4000 samples.

Figure 4.1 corresponds to the MS noise, Figure 4.2 to the SS noise and Figure 4.3 to the BG noise. The part (a) of each Figure represents the quantiles of the empirical distribution function with respect to the Gaussian PDF. The part (b) corresponds to the quantiles with respect to the Gaussian-Gaussian mixture. In this last case, the parameters were computed following the MGF method using the whole window (4000 samples).

The curves seem to be symmetric, except for the SS noise, which indicates odd moments (skewness) greater than normal for this last noise. A problem with the tails can be seen from the somewhat random nature of the curves at the ends, which may be due to the errors in the generation of the Gaussian-Gaussian mixture samples using an IMSL subroutine.

Figure 4.1 shows that the MS noise appears to be adequately described by a Gaussian-Gaussian mixture, the curve in Figure 4.1(b) being more linear than 4.1(a), excepts for the tails. The tails of Figure 4.2 indicates the curious aspect of the SS noise, presenting in both curves a linear central part but irregular tails. The BG noise appears very regular. Both curves of Figure 4.3 are linear with almost no problems at the tails for Figure

4.3(a). In fact, the Gaussian-Gaussian mixture estimate for this case is very close to a Gaussian PDF, c.f. Table III.

4.4. Conclusion

We have studied three underwater noises in this section. One (SS) is non-stationary, apparently because of the presence of impulses. One (BG) appears to be close to Gaussian. Finally, one (MS) seems to be well described by a Gaussian-Gaussian mixture model.

We now study this last noise in the sequel, emphasizing the receiver structure and the normalization necessary to detect a signal in this noise environment.

5. NORMALIZATION FOR THE MIXTURE CASES

For the detection of a signal, say \mathbf{s} , in noise, when the noise amplitude is unknown or time-varying, which is often the case, a power *normalization* is usually incorporated into the receiver in order to regulate the false alarm probability. The noise model can be seen as $\mathbf{x} = a \mathbf{y}$, where \mathbf{x} is the observed noise, \mathbf{y} is a random vector representing the *standardized* noise (zero-mean and unit-variance), and a is a scale-factor, a positive unknown parameter, possibly time-varying, representing the noise amplitude.

With such a model, it is possible to show that every statistic of the form $S(\frac{1}{a} \mathbf{x})$ has a PDF independent of a . Hence, a receiver using such a statistic can be normalized⁽²⁾ [3]. The normalization is done by including in the receiver structure a term which divides the observation by the noise amplitude estimate. More precisely, if $T(\mathbf{x})$ is the optimal test-function associated with a noise of unit-variance, $T(\frac{1}{a} \mathbf{x})$ will be the

(2) In fact, the normalization is exact only if a is known without error, which is usually not the case. In general, the receiver has only a *quasi-normalized adaptive* version, because the parameter a must be estimated from the observation (*adaptive*) and is then known with error (*quasi-normalized*).

optimal test-function associated with a noise with the same distribution but with amplitude -or scale factor- a (or power a^2).

In the sequel, we study the different possible noise amplitude maximum likelihood estimates, calculated either under H_0 or under H_1 . In the latter case, the estimate has the NAR property [17].

5.1. Principle

The PDF of the noise is no longer $P(\mathbf{x})$, standardized (unit-variance), but $Q(\mathbf{x})$, defined by

$$Q(\mathbf{x}) = \frac{1}{a^n} P\left(\frac{1}{a} \mathbf{x}\right), \quad (5.1)$$

where a is the noise amplitude. In this expression, \mathbf{x} is the current observation vector, usually of length equal to that of the signal we want to detect, say n . $P\left(\frac{1}{a}\mathbf{x}\right)$ can be expressed as a product of univariate densities $p\left(\frac{x_i}{a}\right)$ where x_i is the i -th component of the vector \mathbf{x} , assuming that the noise is white and homogeneous.

(5.1) assumes, of course, that the noise PDF is stationary, or at least quasi-stationary, i.e., can be considered as stationary on the length of \mathbf{x} . This corresponds to a slowly fluctuating noise. Since the SS noise seems to vary in an impulsive manner, this noise will not be studied in terms of normalization.

5.2. Maximum Likelihood Estimates Under H_0

To estimate the noise amplitude, one can use the maximum likelihood approach [3]. Under H_0 , the maximum likelihood estimate of a is obtained by solving the following equation,

$$a_0 = -\frac{1}{n} \frac{\mathbf{x}^t \nabla_{\mathbf{x}} [P\left(\frac{1}{a_0} \mathbf{x}\right)]}{P\left(\frac{1}{a_0} \mathbf{x}\right)}. \quad (5.2)$$

The Gaussian-Gaussian mixture PDF leads to an implicit maximum likelihood amplitude estimate of a_{0m} :

$$a_{0m}^2 = \frac{1}{n} \sum_{i=1}^n x_i^2 \frac{(1-\epsilon) \frac{g(x_i/a_{0m};\sigma_1)}{\sigma_1} + \epsilon \frac{g(x_i/a_{0m};\sigma_2)}{\sigma_2}}{(1-\epsilon)g(x_i/a_{0m};\sigma_1) + \epsilon g(x_i/a_{0m};\sigma_2)} . \quad (5.3)$$

For ϵ and $1 - \sigma_1$ small, we can make the following approximation to solve for a_{0m} explicitly:

$$a_{0m}^2 \cong \frac{1}{n \sigma_1} \sum_{i=1}^n x_i^2 + \frac{1}{n} \sum_{i=1}^n x_i^2 \left[\left(\frac{1}{\sigma_1} - 1 \right) \eta_1 \left(\frac{x_i}{a_{0m}} \right) + \epsilon \eta_2 \left(\frac{x_i}{a_{0m}} \right) \right] , \quad (5.4)$$

where

$$\eta_1 \left(\frac{x_i}{a_{0m}} \right) \triangleq \frac{g \left(\frac{x_i}{a_{0m}} ; \sigma_1 \right)}{(1-\epsilon)g \left(\frac{x_i}{a_{0m}} ; \sigma_1 \right) + \epsilon g \left(\frac{x_i}{a_{0m}} ; \sigma_2 \right)} , \quad (5.5)$$

and

$$\eta_2 \left(\frac{x_i}{a_{0m}} \right) \triangleq \frac{g \left(\frac{x_i}{a_{0m}} ; \sigma_2 \right)}{(1-\epsilon)g \left(\frac{x_i}{a_{0m}} ; \sigma_1 \right) + \epsilon g \left(\frac{x_i}{a_{0m}} ; \sigma_2 \right)} . \quad (5.6)$$

Hence, an approximation of a_{0m}^2 can be found by replacing a_{0m}^2 on the right hand of (5.3) by $\frac{1}{n \sigma_1} \sum_{i=1}^n x_i^2$. This is the method used in the simulations presented here ⁽³⁾.

The maximum likelihood estimate calculated under H_0 for a Gaussian PDF is

$$a_{0g}^2 = \frac{1}{n} \mathbf{x}^t \mathbf{x} , \quad (5.7)$$

the standard power estimate.

(3) This approach can also be used to compute a_{0m} recursively.

Figure 5.1 represents the maximum likelihood power estimate a_{0m}^2 , given by the approximation of (5.3), and a_{0g}^2 , given by (5.7) for the MS noise. These estimates have been computed on windows of length 100 samples. This length represents 80 ms which is the duration of a classical active sonar signal. We observe that the difference between the two curves is negligible. We think that the reason for this is that this noise, although not Gaussian, is not far from Gaussian. Hence, the use of a_{0g} instead of a_{0m} leads to essentially the same result and is easier to implement.

5.3. Detection and N A R Estimate

The previous estimates were calculated under H_0 , i.e., the assumption that the observations were composed only of noise. In a typical detection problem, a signal can be present in this observation and its presence must not affect the amplitude estimate in order to avoid a normalization of the signal by itself [18]. The amplitude estimate must be a Noise Alone Reference [17], i.e., be insensitive to the possible presence (or absence) of a signal.

It is possible to obtain the maximum likelihood estimate of the noise amplitude under the hypothesis H_1 [3], by solving the following implicit equation,

$$a_1 = -\frac{1}{n} \frac{\mathbf{x}^t \nabla_{\mathbf{x}} [P(\frac{1}{a_1}(\mathbf{x}-\mathbf{s}))]}{P(\frac{1}{a_1}(\mathbf{x}-\mathbf{s}))} . \quad (5.8)$$

In the Gaussian case, this leads to the NAR estimate,

$$a_{1g}^2 = \frac{1}{n} \left(\mathbf{x}^t \mathbf{x} - \frac{(\mathbf{s}^t \mathbf{x})^2}{\mathbf{s}^t \mathbf{s}} \right) . \quad (5.9)$$

In the mixture case, the previous implicit equation is not easily solvable. Consequently, we use an approximation which consists of replacing \mathbf{x} by its projection onto the sub-

space of the observation space orthogonal to the signal \mathbf{s} to be detected [19]. This is accomplished by using

$$\mathbf{y} = \mathbf{x} - \frac{\mathbf{s}^t \mathbf{x}}{\mathbf{s}^t \mathbf{s}} \mathbf{s}, \quad (5.10)$$

instead of \mathbf{x} . We have used this approach to get a NAR amplitude estimate, say a_{1m} , for the mixture case, replacing x_i by y_i in (5.3)-(5.6).

5.4. Test-Functions and R O C Curves

We will use two types of receiver structures. The first one corresponds to the white Gaussian noise assumption and is the matched filter in white noise, $\mathbf{s}^t \mathbf{x}$. The second one corresponds to a processor associated with the mixture assumption and will be denoted by $L_m(\mathbf{x})$,

$$L_m(\mathbf{x}) = \prod_{i=1}^n \frac{(1-\epsilon)g(x_i - s_i; \sigma_1) + \epsilon g(x_i - s_i; \sigma_2)}{(1-\epsilon)g(x_i; \sigma_1) + \epsilon g(x_i; \sigma_2)}. \quad (5.11)$$

As previously noted, instead of using \mathbf{x} in these two structures, we have to use $\frac{1}{a} \mathbf{x}$ as the input to the receiver. Of course, a is not known exactly and will be replaced by an estimate. We can use the estimate calculated under either H_0 or H_1 , and corresponding to either a Gaussian or a mixture assumption. These four estimates are a_{0g} , a_{1g} for the Gaussian case, and a_{0m} , a_{1m} for the mixture case. The subscript 1 corresponds to the NAR estimate. The test-functions are

$$t_g(\mathbf{x}) = \frac{\mathbf{s}^t \mathbf{x}}{a_{0g}}, \quad (5.12)$$

$$T_g(\mathbf{x}) = \frac{\mathbf{s}^t \mathbf{x}}{a_{1g}}, \quad (5.13)$$

$$t_m(\mathbf{x}) = L_m\left(\frac{\mathbf{x}}{a_{0m}}\right), \quad (5.14)$$

$$T_m(\mathbf{x}) = L_m\left(\frac{\mathbf{x}}{a_{1m}}\right). \quad (5.15)$$

In these expressions, we have been consistent by using the same assumption for the receiver and the normalization structures, Gaussian with Gaussian, mixture with mixture.

Using a standard Monte-Carlo method, R O C curves have been computed for these test-functions using the MS noise. The results are indicated in Figures 5.2 and 5.3. These figures represent the probability of detection with respect to the probability of false alarm for the four previous test-functions.

Each “number” in these curves corresponds to a point associated with one threshold, say t , for the corresponding receiver, in the sense that if the output is greater than t , the hypothesis H_1 , *signal present*, is chosen, whereas if it is smaller than t , we decide H_0 , *noise only*. 100,000 observations vectors have been used for each curve, in order to get the probabilities of false alarm and detection.

The signal have been taken either constant, Figure 5.2, or pseudo-random (white noise sequence), Figure 5.3. In both cases, the signal-to-noise ratio was 0 dB at the receiver input. The probability of false alarm is represented through its logarithm in basis 10. The curve noted “1” corresponds to the receiver $t_g(\cdot)$, (5.12), the one noted “2” corresponds to the receiver $T_g(\cdot)$, (5.13), and so on, “3” for $t_m(\cdot)$, (5.14), and “4” for $T_m(\cdot)$, (5.15).

We note that we obtain the same kind of qualitative results while using the BN noise instead of the MS noise. The differences between the two types of receiver is smaller than for the MS noise. This is due to the fact that the BN noise, as previously observed, is closer to a Gaussian noise than the MS noise.

In a previous study [3], it was shown analytically that since $t_g(\cdot)$ and $T_g(\cdot)$ are

monotonically related, they have the same ROC curves, but not the same deflection criterion. Here, we empirically verify this observation for the ROC curves. The test-function $t_m(\cdot)$, (5.14), gives the best results in both cases. This would seem to indicate that the Gaussian-Gaussian mixture model is closer to the real underlying density than the Gaussian PDF. This is true even with a very simple parameter estimation procedure; in effect, the parameters of the mixture model, ϵ , σ_1 , and σ_2 , have been computed on the whole window (4000 samples). Small variations can occur from a small window (20 samples) to another and we have computed an estimate based on a global model, not necessarily consistent with each local window. Even with this approximation, made in order to simplify the processing and to test the performance of a *static* (not adaptive) mixture model, the results are quite good.

The test-function $T_m(\cdot)$, (5.15), leads to results very close to those of $t_m(\cdot)$. As in the Gaussian case, there is no difference between these two test-functions in the constant signal case, Figure 5.2. The very small difference between the two curves corresponding to the mixture receiver and observed for the pseudo-random signal case, Figure 5.3, can be explained by the sensitivity to poor estimates and/or effects of approximations in the computation of the NAR reference. We have also made an approximation in order to compute the amplitude estimates associated with the mixture. If a NAR estimate is desired, the one based on the Gaussian assumption may be more tolerant to errors and less sensitive to approximations and deviations from the true density than the one based on the mixture assumption.

6. COMPARISON OF ADAPTIVE/ROBUST RECEIVERS

In this section we are going to compare three receivers, without any different normalization; the previous section has shown that the type of normalization used (under H_0 or H_1) has no importance on the performance in term of ROC curves. Assuming the

noise white and stationary, we are going to study the *adaptive* receiver corresponding to the likelihood ratio for the Gaussian-Gaussian mixture and two *robust* receivers, matched filter and soft-limiter. The matched filter is robust with respect to the relative efficiency [9,20]. The soft-limiter is robust with respect to the ROC curves [21]. For the purpose of comparison, the non-linearities of these three different receivers are represented on Figure 6.1. We have used the optimal receiver (5.11) associated with the mixture, and not the locally-optimal one for the simulations.

ROC curves have been computed for different values of the parameters. They are represented on Figures 6.2 to 6.13. Each curves corresponds to the three receivers previously mentioned, "1" being associated to the matched filter, "3" to the mixture likelihood ratio, "5" to the soft-limiter. 100,000 samples of the MS noise have been used for SNR of 0, -5 and -10 dB, (10,000 samples only for -15 dB). Three different threshold values (k) for the soft-limiter have been used, 1.4, 2.0 and 2.5. The noise variance was 1.

The following preliminary conclusions can be made. First, the mixture receiver always ⁽⁴⁾ performs better than the matched filter which, in turns, is better than the soft-limiter. At 0 dB, from Figures 6.2, 6.6 and 6.10, the matched filter is seen to have almost the same performance as the mixture receiver until a PFA of 10^{-4} . This can be explained by the fact that, for this high SNR situation, we are in a *linear* area of the mixture non-linearity, i.e., we are operating in the second linear region for these high inputs, c.f. Figure 6.1. For a SNR of -5 dB, from Figures 6.3, 6.7 and 6.11, we are in the area where this mixture input-output relationship is highly non-linear. Consequently, the degradation between this receiver and the matched filter is more pronounced. At -10 dB, from Figures 6.4, 6.8 and 6.12, the difference decreases because we are around the

(4) except for low probabilities of false alarm, 10^{-3} , 10^{-4} , at -15 dB, but the difference is very small.

origin where the mixture non-linearity becomes more *linear* for small SNR. At -15 dB, from Figures 6.5, 6.9 and 6.13, we see that the three receivers have almost the same performance.

The soft-limiter with the smallest threshold at 1.4, Figures 6.2 to 6.5, has bad performance, even at high SNR where the limitation cuts out most of the signal. The differences between the mixture receiver and the matched filter is usually bigger than the difference between the matched filter and the soft-limiter. This is in particular true for $k = 2.0$ and 2.5 , where the soft-limiter is very close to the matched filter.

These results can be explained by the facts that the MS noise is closer to a Gaussian-Gaussian mixture than to a Gaussian PDF, as seen in the previous section, and that it has no impulsive components. Consequently, the soft-limiter cuts the signal and not the noise, especially at high SNR. At low SNR, the total observation has, in general, small amplitudes such that we are in the area around zero. This is the area where the three non-linearities are almost the same, c.f. Figure 6.1. Hence, the three receivers perform nearly the same at low SNR.

7. CONCLUSION

Three underwater acoustical noises samples have been studied with emphasis on noise PDF modeling. The SS noise, generated mostly by biological phenomenon, appears to be non-stationary. The BG noise is very close to Gaussian. The MS noise seems to be adequately described by a Gaussian-Gaussian mixture. This last noise has also been studied in a detection framework with a normalization of the receiver necessary to obtain a constant false alarm rate.

The noise power maximum likelihood estimates under H_0 or H_1 assuming a Gaussian PDF give very similar results. If a signal is to be detected in a noise close to the

mixture model, the use of a receiver associated with the Gaussian-Gaussian assumption (receiver structure and normalization) appears to have better performance in terms of ROC curves than those corresponding to a Gaussian model. This is an indication of a better fitting of the mixture model to the data. In both cases, the use of the NAR noise power estimate leads to the same performance as the use of a *standard* one, calculated under H_0 .

Finally, the Gaussian-Gaussian mixture likelihood ratio receiver, considered as an *adaptive* receiver, has been shown to have better performance than two *robust* receivers, the matched filter and the soft-limiter.

APPENDIX A

Assume a PDF modeled by (3.4), with zero-mean and unit-variance. A method of moment estimation permits quite easily the calculation of the three relevant parameters. Since the variance is one, and denoting by e_4 and e_6 the fourth and sixth moments of the observation, we have

$$(1-\epsilon) \sigma_1^2 + \epsilon \sigma_2^2 = 1, \quad (\text{A.1})$$

$$(1-\epsilon) \sigma_1^4 + \epsilon \sigma_2^4 = \frac{e_4}{3}, \quad (\text{A.2})$$

$$(1-\epsilon) \sigma_1^6 + \epsilon \sigma_2^6 = \frac{e_6}{15}. \quad (\text{A.3})$$

Assuming $\epsilon \ll 1$, and $e_4 < 3$, we can get these parameters in a straightforward manner:

$$\sigma_1^2 \cong \sqrt{\frac{e_4}{3}}, \quad (\text{A.4})$$

$$\sigma_2^2 \cong \left[\frac{e_6}{15(1-\sqrt{e_4/3})} \right]^{\frac{1}{2}}, \quad (\text{A.5})$$

$$\epsilon \cong \sqrt{\frac{e_6}{15}} \left(1 - \sqrt{\frac{e_4}{3}} \right)^{\frac{3}{2}}. \quad (\text{A.6})$$

APPENDIX B

The idea of the Moment Generating Function method is to minimize the mean square error in the estimate of the generating function, $E \{ e^{\theta x} \}$:

$$e^2(\theta, \gamma) = \sum_{j=1}^k |G(\theta_j) - F(\gamma, \theta_j)|^2, \quad (\text{B.1})$$

where

$$G(\theta) = \frac{1}{N} \sum_{i=1}^N e^{\theta x_i} \quad (\text{B.2})$$

is the empirical generating function, x_i being the i -th sample of the observation composed of N samples;

$$\theta = [\theta_1, \theta_2, \dots, \theta_k]^t \quad (\text{B.3})$$

is a vector of k values;

$$\gamma = [\epsilon, \sigma_1, \sigma_2]^t \quad (\text{B.4})$$

is the vector of the Gaussian-Gaussian mixture parameters;

$$F(\gamma, \theta) = (1-\epsilon) e^{\frac{1}{2}\sigma_1^2\theta^2} + \epsilon e^{\frac{1}{2}\sigma_2^2\theta^2} \quad (\text{B.5})$$

is the generating function associated with the mixture model.

In the simulation presented in this paper, we have used $N = 4000$ for the whole window (or 2000 for the smaller ones), $k = 3$, $\theta = [0.1, 0.4, 0.8]^t$, and a gradient method for the minimization of the square error, initialized with the results of the MOM method for the mixture.

This method has been chosen because of its good results as described in a previous paper [16], and as discussed by others in comments following that paper.

REFERENCES

- [1] HELSTROM C.W. : "Statistical theory of signal detection", Pergamon Press, 1968
- [2] VAN TREES H. : "Detection, estimation and modulation theory", Part I, John Wiley, 1968
- [3] BOUVET M., PICINBONO B. : "Adaptive normalization and detection", *Proceedings of ICC 85*, Chicago, 23-26 June 1985
- [4] SCHWARTZ S. C., THOMAS J. B. : "Detection in a non- Gaussian environment", in *Statistical signal processing*, WEGMAN E. J., SMITH J.G. (editors), Marcel Decker, 1984, pp. 93-105
- [5] CZARNECKI S.V., THOMAS J.B. : "Nearly optimal detection of signals in non-Gaussian noise", *Information Sciences and Systems Laboratory Report no 14*, Princeton University, February 1984
- [6] WILSON G. R., POWELL D. R. : "Experimental and modeled density estimates of underwater acoustic returns", *Proceedings of Signal Processing in the Ocean Environment Workshop*, Annapolis (MD), May 1982
- [7] MIDDLETON D. : "Statistical-physical models of electromagnetic interference", *IEEE Transactions on EC*, vol 19, no 3, August 1977, pp. 106-127
- [8] MIDDLETON D. : "Procedures for determining the parameters of the first order canonical model of class-A and class B electromagnetic interference", *IEEE Transactions on EC*, vol 21, no 3, August 1979, pp. 190-208
- [9] VASTOLA K. S. : "Threshold detection in narrow-band non-Gaussian noise", *IEEE Transactions on Communications*, vol 32, no 2, February 1984, pp. 134-139
- [10] F.W. MACHELL, C.S. PENROD : "Probability density functions of ocean acoustic noise processes", in *Statistical signal processing*, WEGMAN E. J., SMITH J.G. (editors), Marcel Decker, 1984, pp. 211-221
- [11] VEITGH J.G., WILKS A.R. : "A characterization of arctic undersea noise", *JASA*, vol 77, no 3, March 1985, pp. 989-999
- [12] DWYER R. : "Use of the kurtosis statistic in the frequency domain as an aid in detecting random signal", *IEEE Trans. on Oceanic Engineering*, vol 9, no 2, April 1984, pp. 85-92
- [13] SCHARF L.L., LYTLE D.W.: "Signal detection in Gaussian noise of unknown level: a invariance application", *IEEE Transactions on IT*, vol 17, no 4, July 1971, pp. 404-411
- [14] SWASZEK P.F., EFRON A.J., TUFTS D.W.: "Detection based on the mixture model", *Proceedings of the 1985 John Hopkins Conference on Information Science and Systems*, March 1985
- [15] POWELL D.R., WILSON G.R. : "Class A modeling of ocean acoustic noise processes", to be published.
- [16] R.E. QUANDT, J.B. RAMSEY : "Estimating mixtures of normal distributions and switching regressions", *J. of American Statistical Ass.*, vol 73, no 364, December 1978, pp. 730-752
- [17] EL AYADI M.H., PICINBONO B. : "N A R AGC adaptive detection of non-overlapping signals in noise with fluctuating power", *IEEE Trans. on ASSP*, vol 29, no 5, October 1981, pp. 952-963

- [18] TACCONI E., BOUVET M., PICINBONO B. : "A new N A R power estimator for adaptive detection", *Proceedings of ICASSP 84* , San Diego, 19-21 March 1984
- [19] PICINBONO B. : "A geometrical interpretation of signal detection and estimation", *IEEE Trans. on IT* , vol 26, no 4, July 1980, pp. 493-497
- [20] BOUVET M.: "Expansions of the likelihood ratio and application", submitted to the *IEEE Transactions on ASSP*
- [21] MARTIN R.D., SCHWARTZ S.C.: "Robust detection of a known signal in nearly Gaussian noise", *IEEE Transactions on IT*, vol 17, no 1, January 1971, p 50-56

TABLES

- I *Results for the MC noise*
- II *Results for the SS noise*
- III *Results for the BG noise*

FIGURES

- 2.1 *Merchant Ship Noise: observation*
- 2.2 *Merchant Ship Noise: mean on 20 samples*
- 2.3 *Merchant Ship Noise: variance on 20 samples*
- 2.4 *Snapping Shrimp Noise: observation*
- 2.5 *Snapping Shrimp Noise: mean on 20 samples*
- 2.6 *Snapping Shrimp Noise: variance on 20 samples*
- 2.7 *Background Noise: observation*
- 2.8 *Background Noise: mean on 20 samples*
- 2.9 *Background Noise: variance on 20 samples*
- 4.1 *Quantiles for the MS noise: (a) Gaussian reference, (b) Gaussian-Gaussian Mixture reference*
- 4.2 *Quantiles for the SS noise: (a) Gaussian reference, (b) Gaussian-Gaussian Mixture reference*
- 4.3 *Quantiles for the BG noise: (a) Gaussian reference, (b) Gaussian-Gaussian Mixture reference*
- 5.1 *Noise Power Estimates for the MS Noise*
- 5.2 *ROC curves for the MS noise and a constant signal*
- 5.3 *ROC curves for the MS noise and a pseudo-random signal*

- 6.1 *Non-linearities: (a) mixture receiver, (b) matched filter, (c) soft-limiter*
- 6.2 *ROC curves for the MS noise and a constant signal, $k=1.4$, SNR =0 dB*
- 6.3 *ROC curves for the MS noise and a constant signal, $k=1.4$, SNR =-5 dB*
- 6.4 *ROC curves for the MS noise and a constant signal, $k=1.4$, SNR =-10 dB*
- 6.5 *ROC curves for the MS noise and a constant signal, $k=1.4$, SNR =-15 dB*
- 6.6 *ROC curves for the MS noise and a constant signal, $k=2.0$, SNR =0 dB*
- 6.7 *ROC curves for the MS noise and a constant signal, $k=2.0$, SNR =-5 dB*
- 6.8 *ROC curves for the MS noise and a constant signal, $k=2.0$, SNR =-10 dB*
- 6.9 *ROC curves for the MS noise and a constant signal, $k=2.0$, SNR =-15 dB*
- 6.10 *ROC curves for the MS noise and a constant signal, $k=2.5$, SNR =0 dB*
- 6.11 *ROC curves for the MS noise and a constant signal, $k=2.5$, SNR =-5 dB*
- 6.12 *ROC curves for the MS noise and a constant signal, $k=2.5$, SNR =-10 dB*
- 6.13 *ROC curves for the MS noise and a constant signal, $k=2.5$, SNR =-15 dB*

REAL DATA

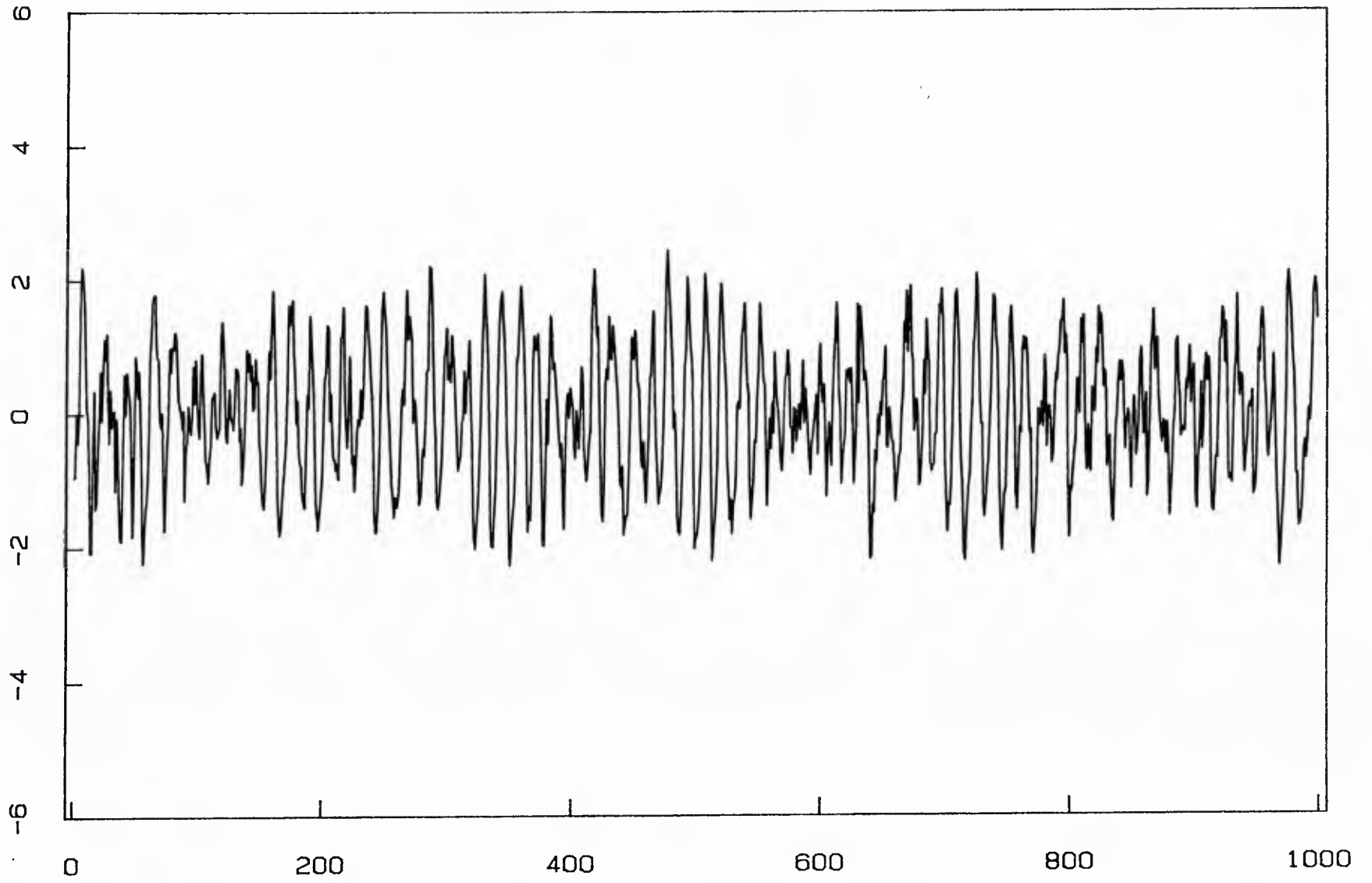


Figure 2.1
Merchant Ship Noise: observation

REAL DATA

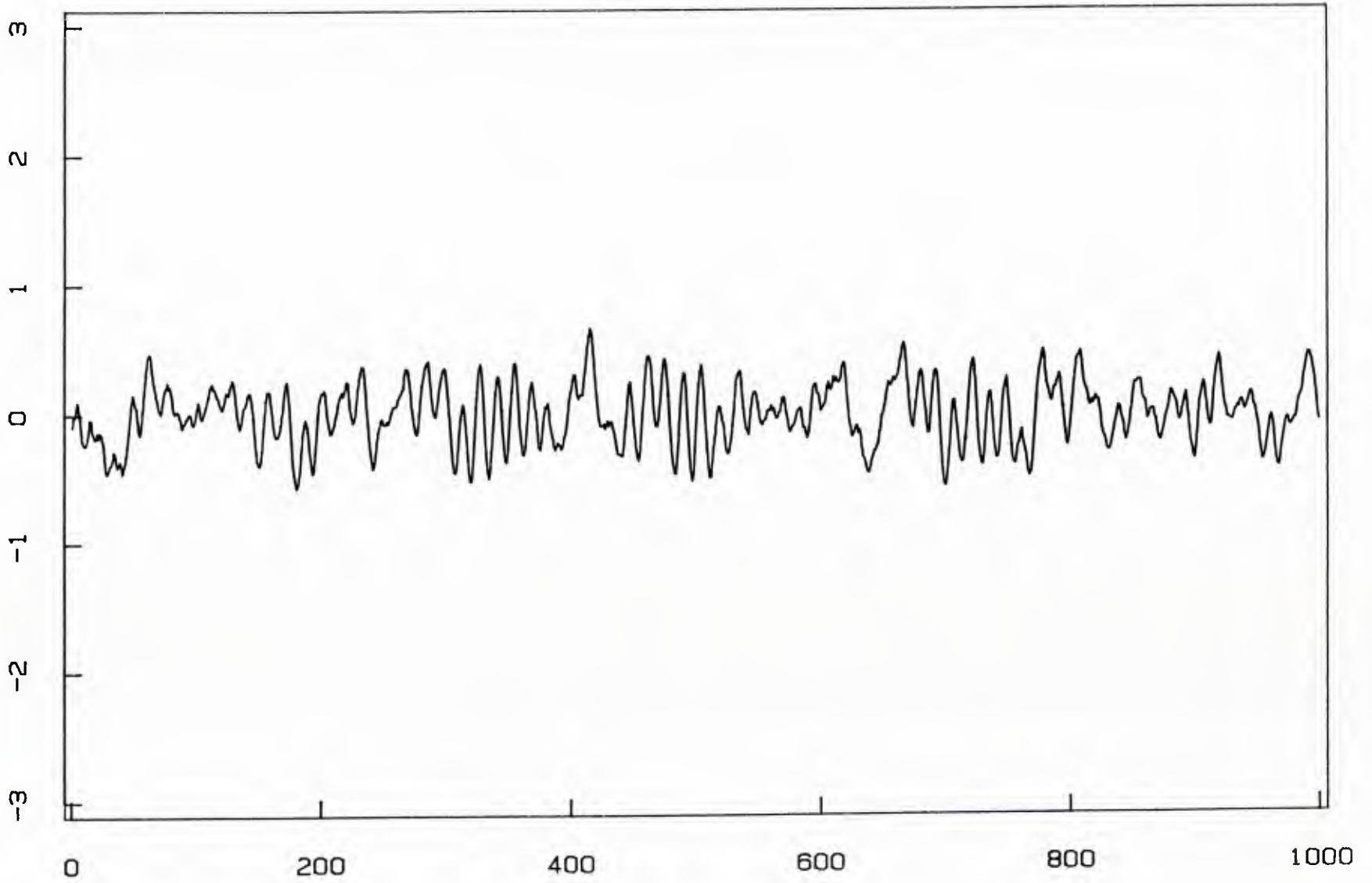


Figure 2.2
Merchant Ship Noise: mean on 20 samples

REAL DATA

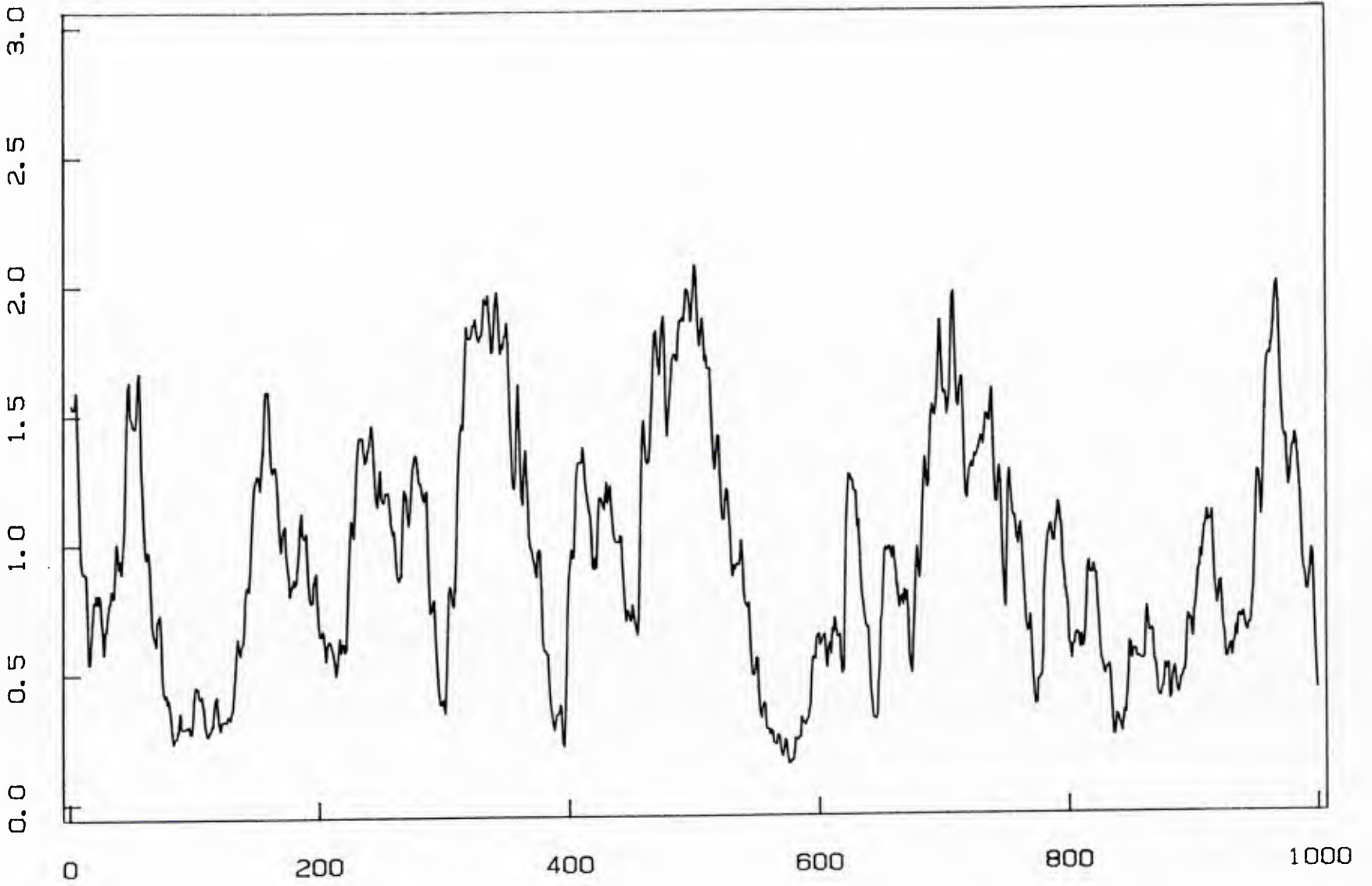


Figure 2.3
Merchant Ship Noise: variance on 20 samples

REAL DATA

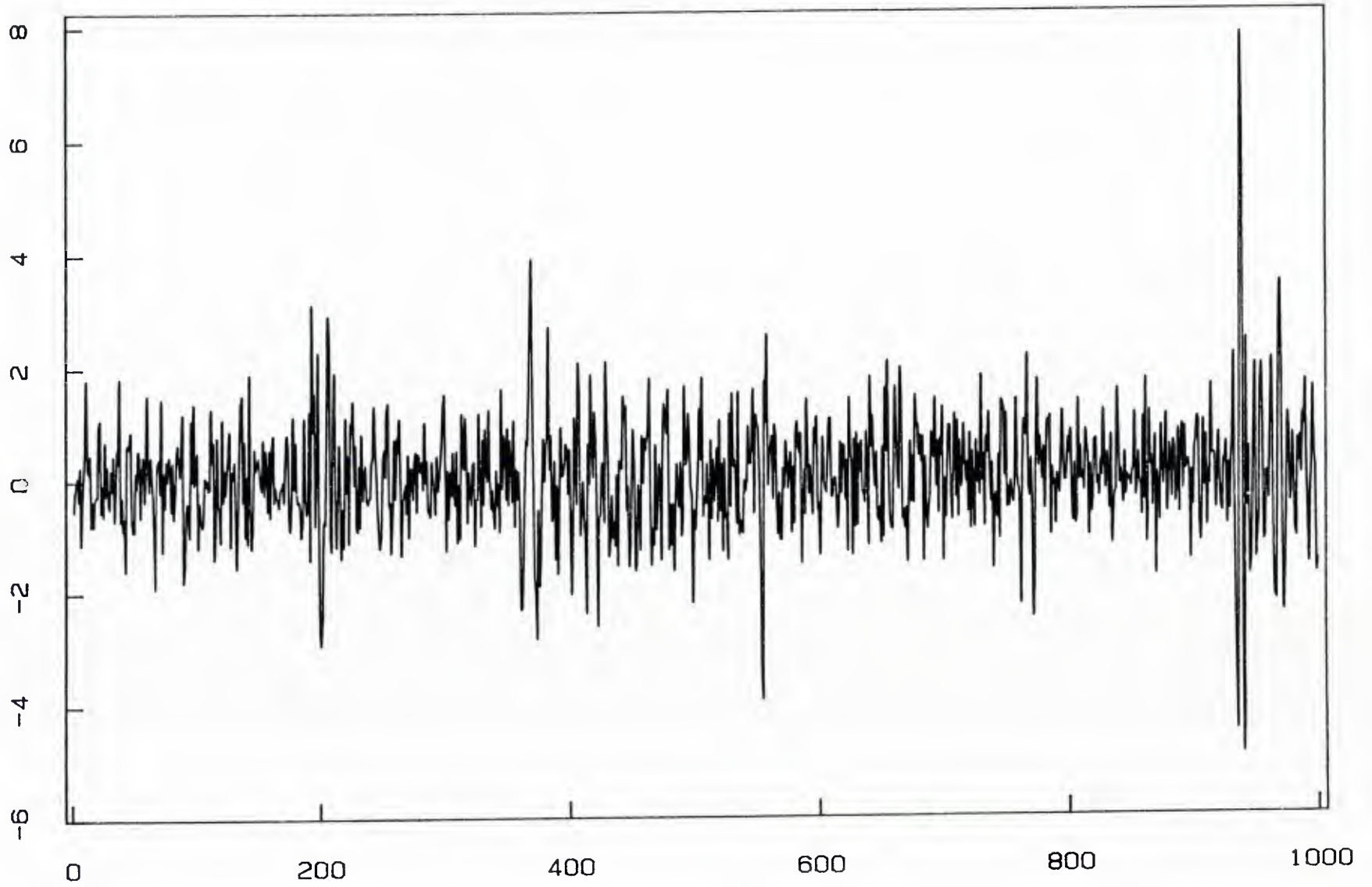


Figure 2.4
Snapping Shrimp Noise: observation

REAL DATA

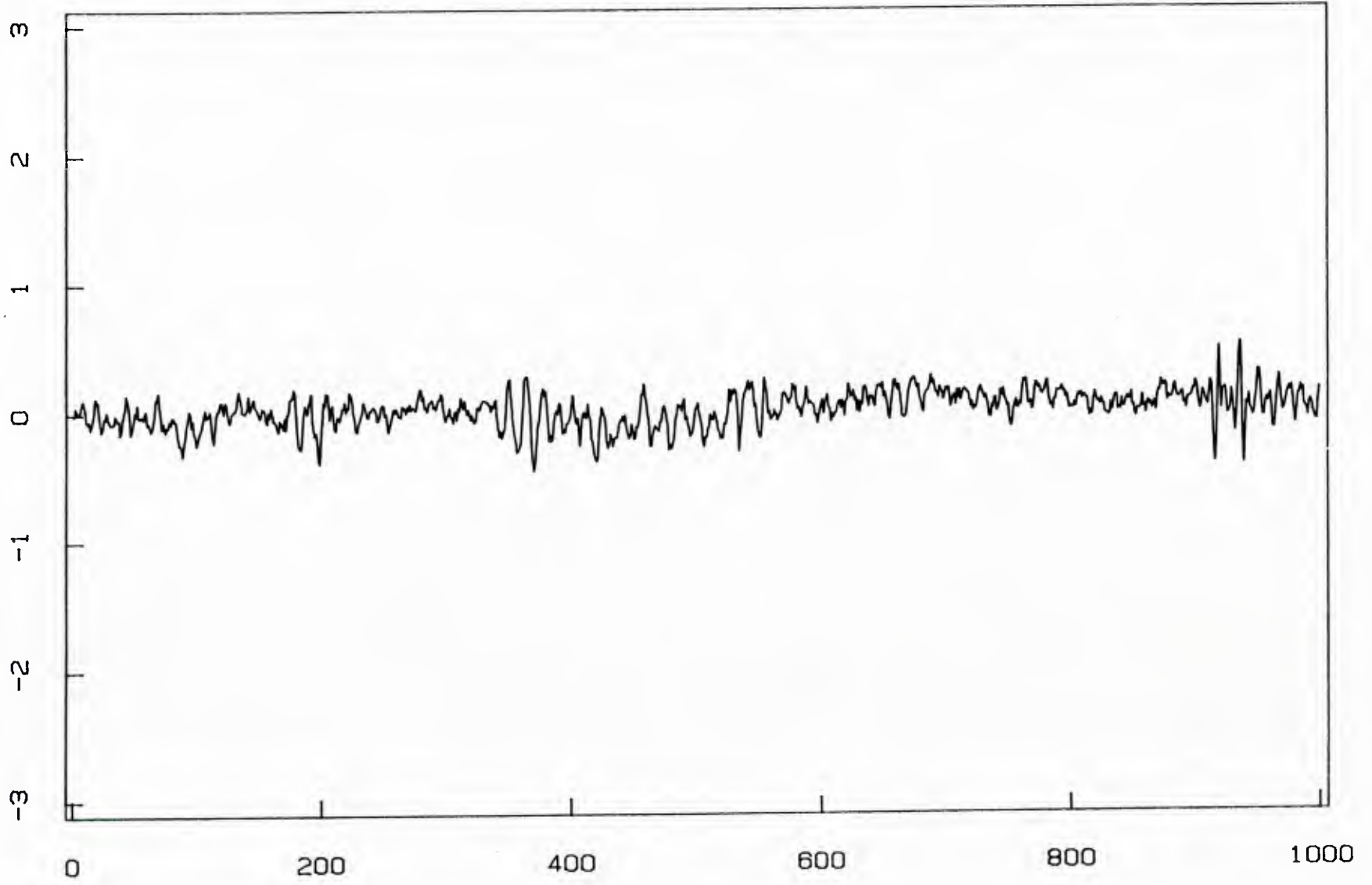


Figure 2.5
Snapping Shrimp Noise: mean on 20 samples

REAL DATA

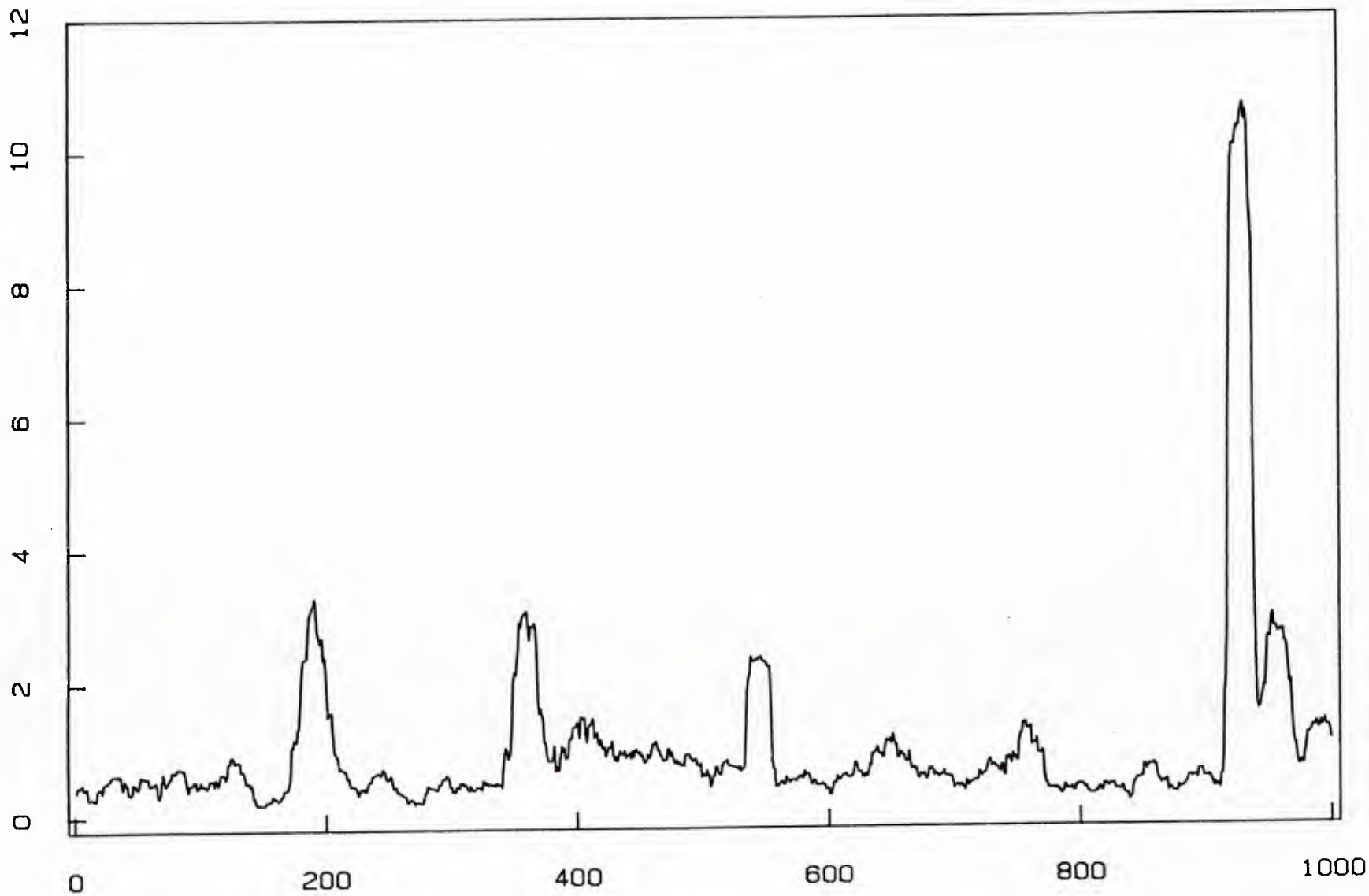


Figure 2.6
Snapping Shrimp Noise: variance on 20 samples

REAL DATA

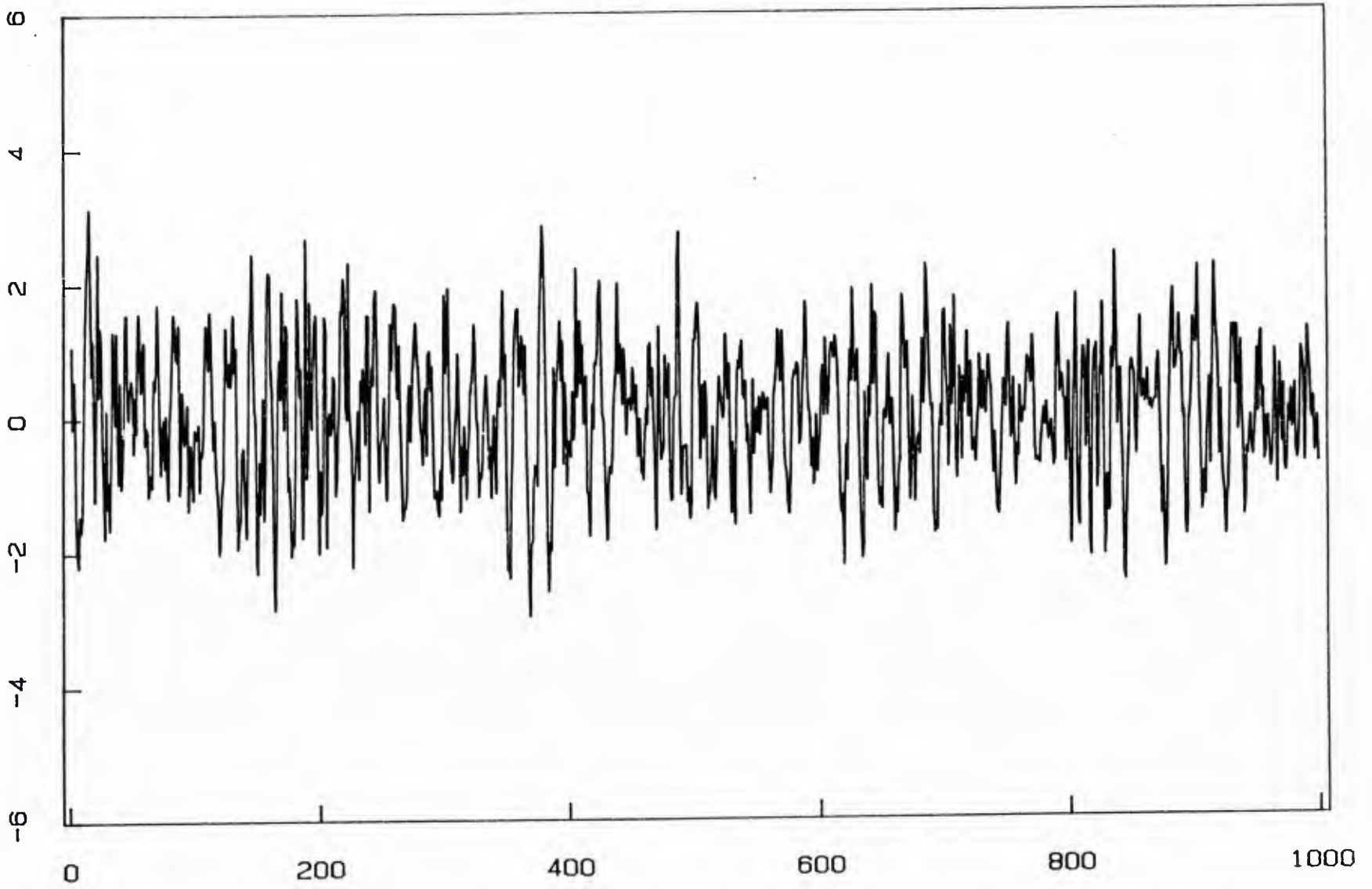


Figure 2.7
Background Noise: observation

REAL DATA

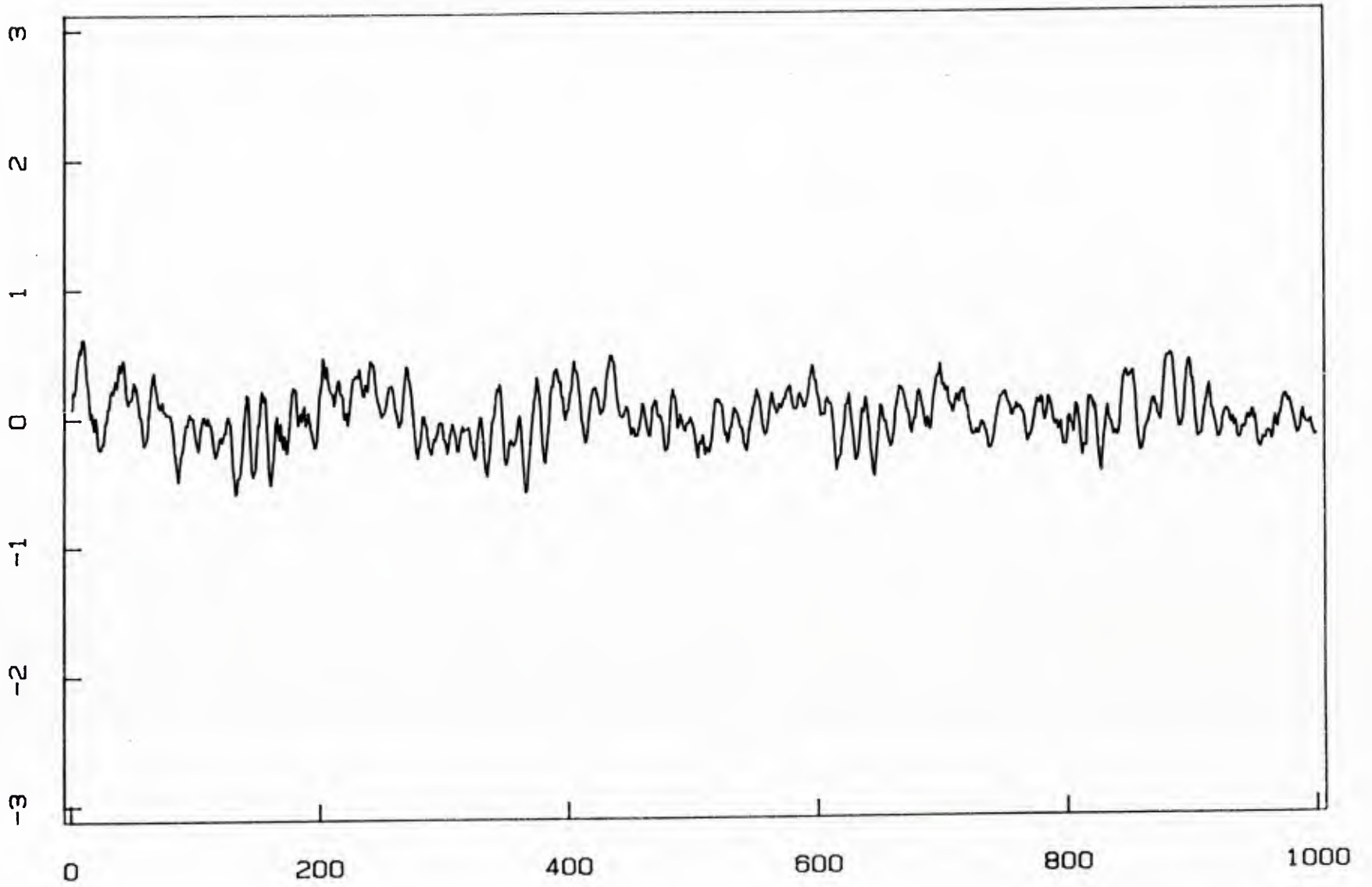


Figure 2.8
Background Noise: mean on 20 samples

REAL DATA

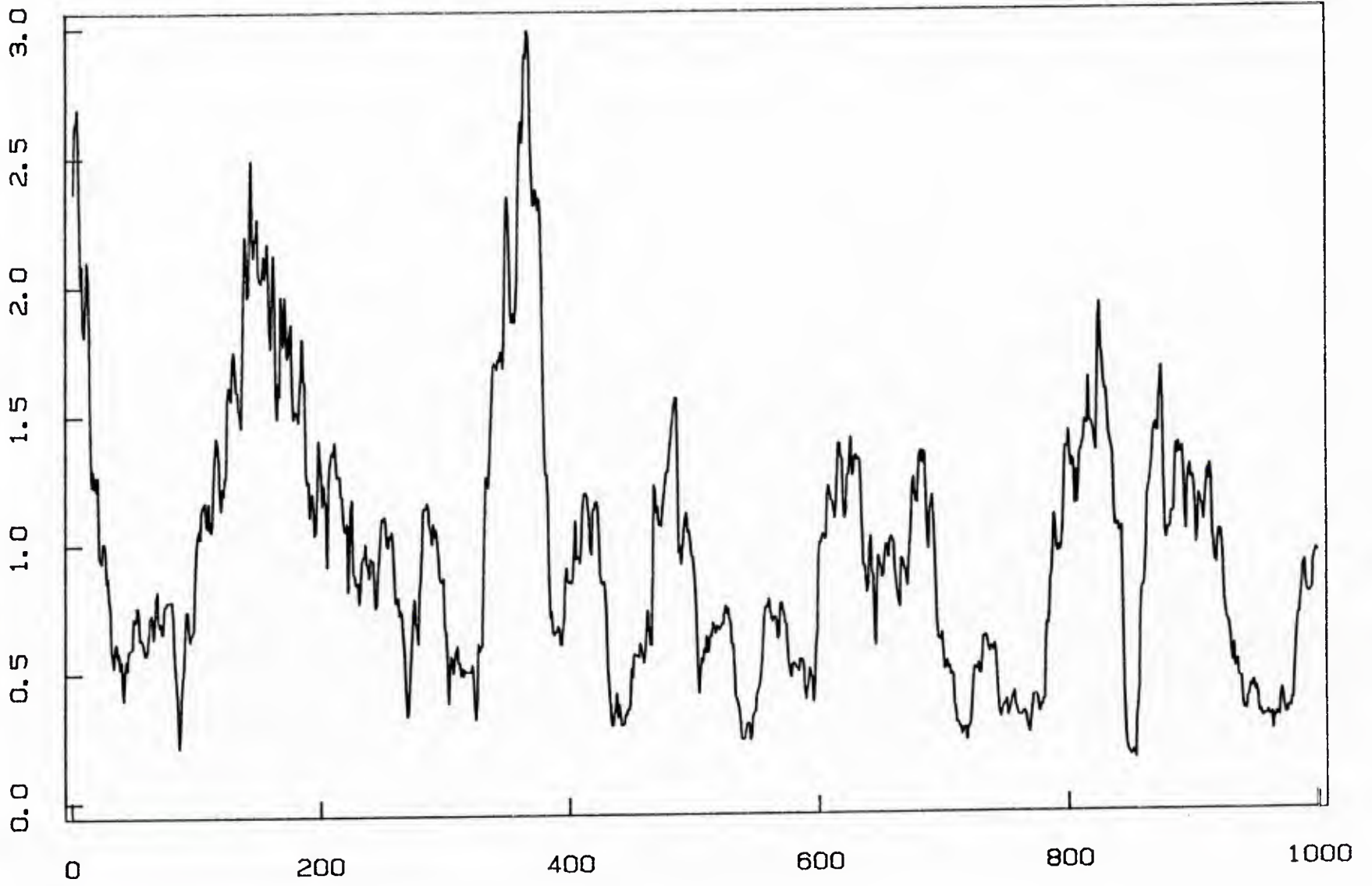


Figure 2.9
Background Noise: variance on 20 samples

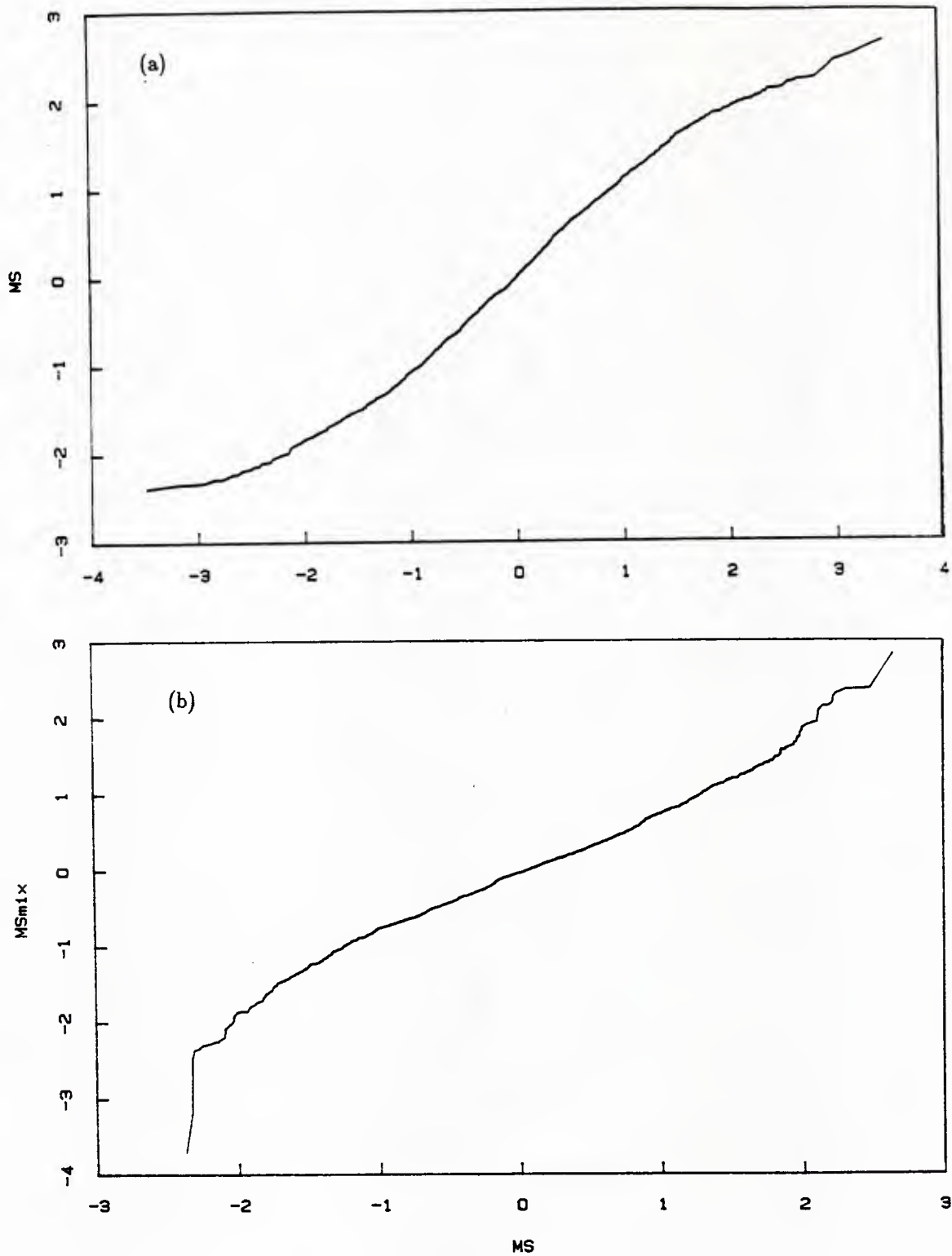


Figure 4.1
Quantiles for the MS noise
(a) Gaussian reference
(b) Gaussian-Gaussian Mixture reference

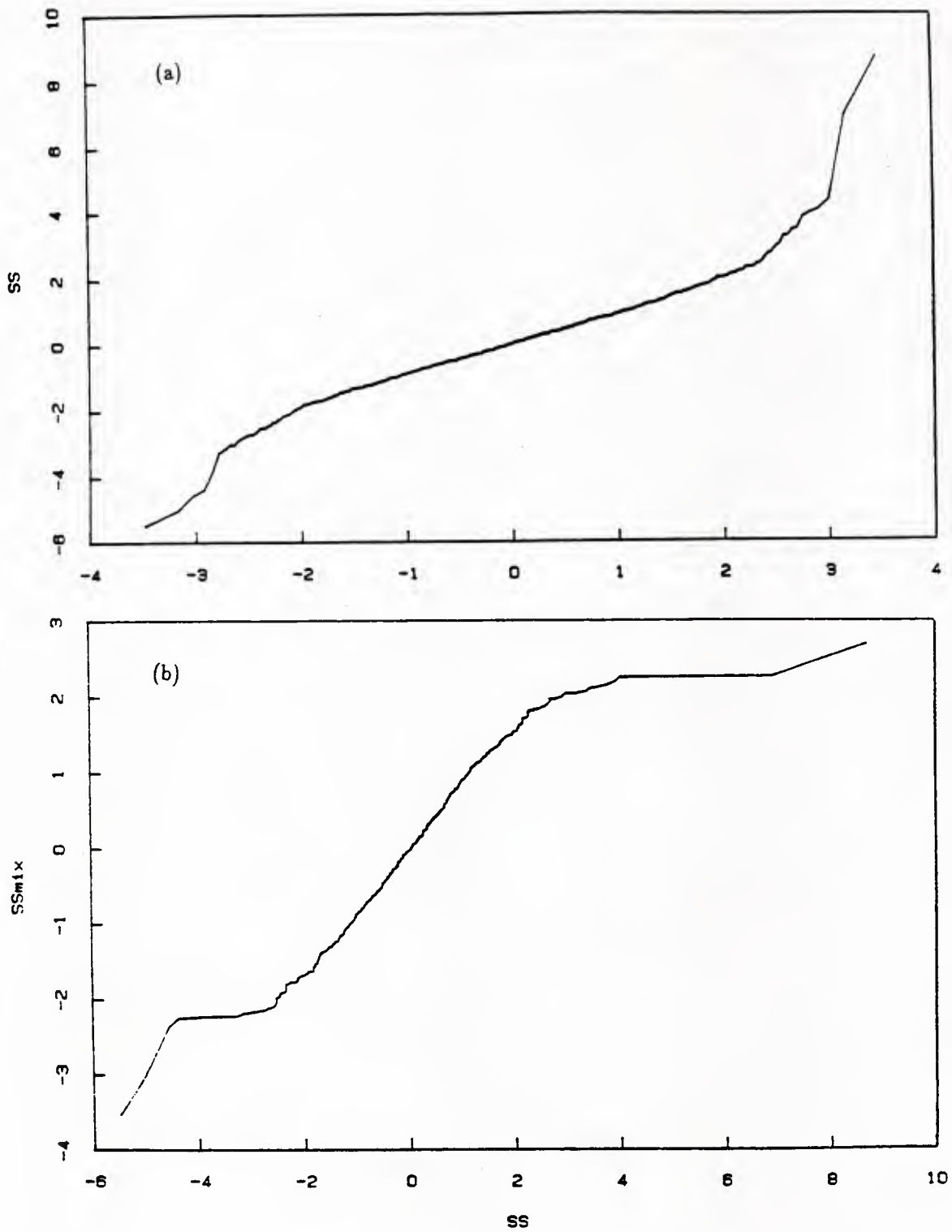


Figure 4.2
Quantiles for the SS noise
(a) Gaussian reference
(b) Gaussian-Gaussian Mixture reference

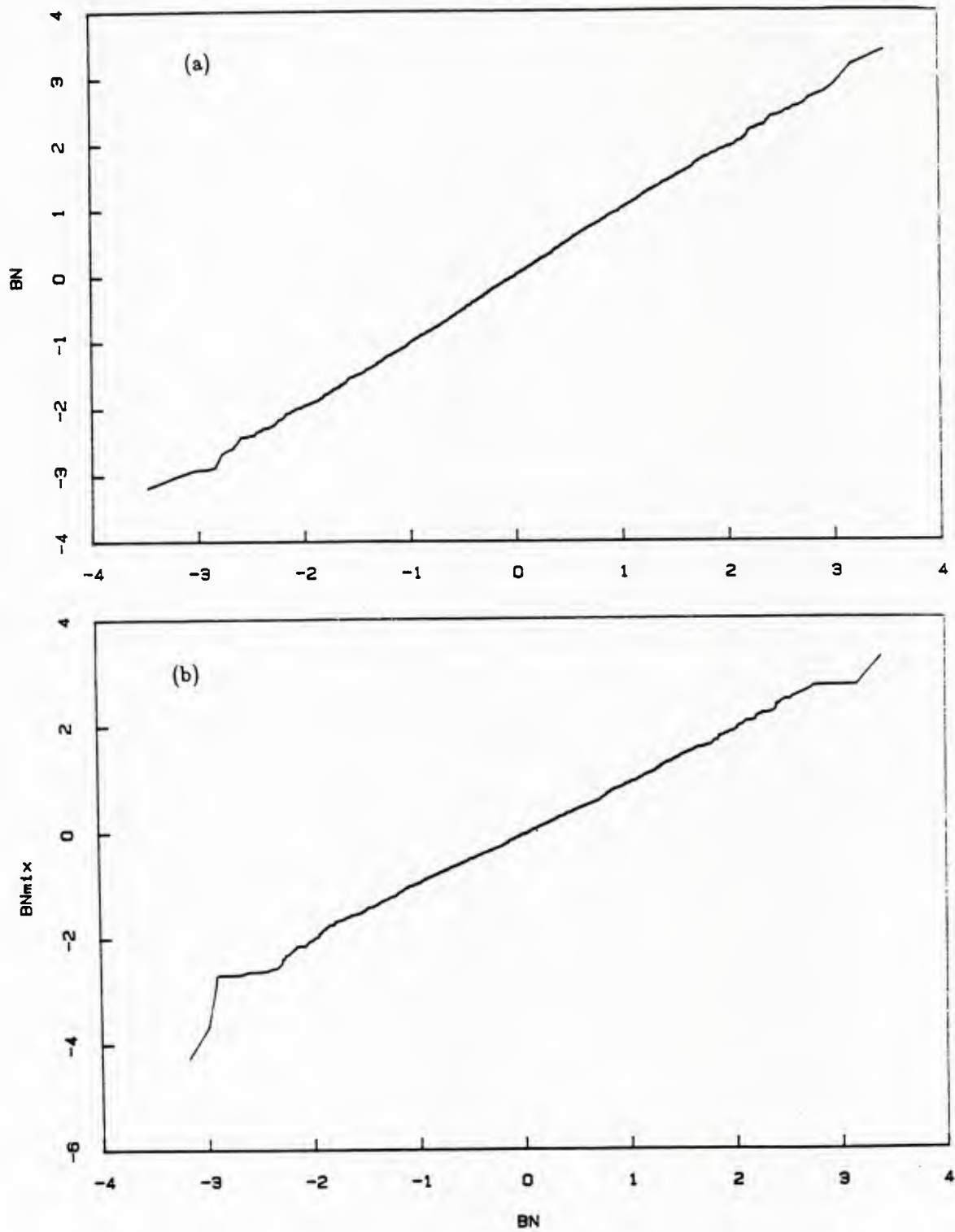
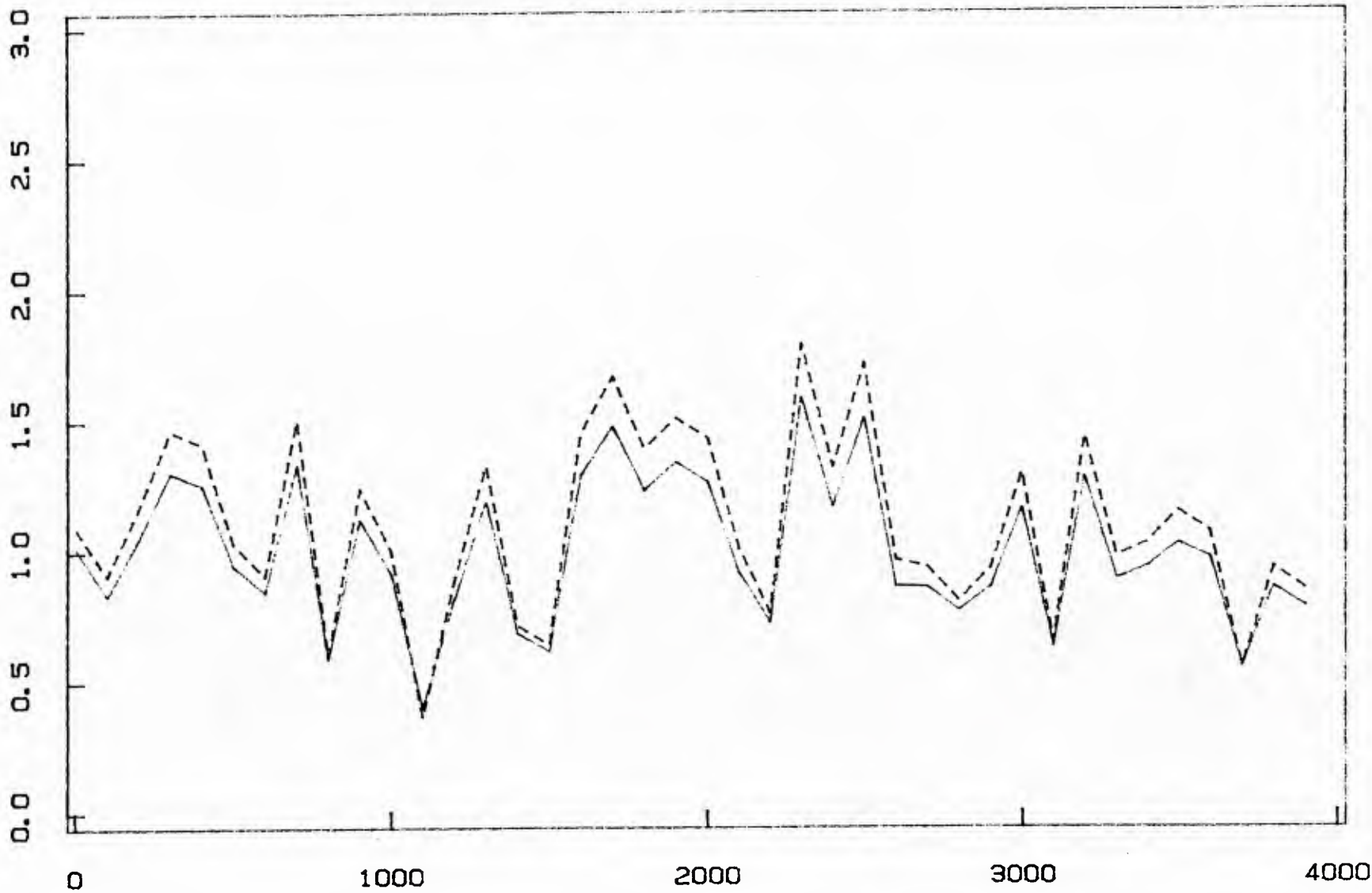


Figure 4.3
Quantiles for the BG noise
(a) Gaussian reference
(b) Gaussian-Gaussian Mixture reference

Figure 5.1
Noise Power Estimates for the MS Noise



STANDARD ESTIMATE — . MAXIMUM LIKELIHOOD ESTIMATE ----
WINDOW LENGTH : 100 SAMPLES

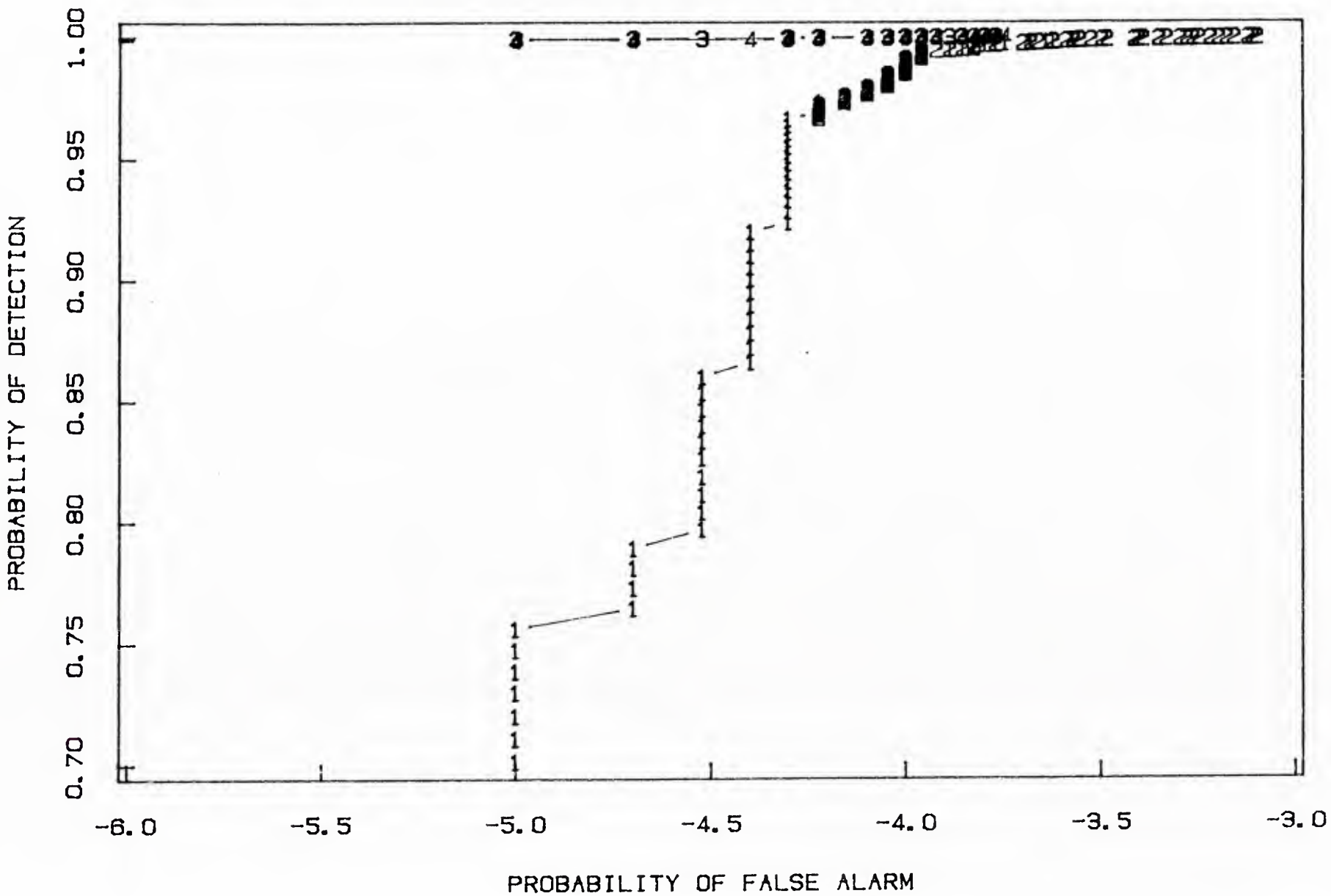


Figure 5.2
 ROC curves for the MS noise and a constant signal

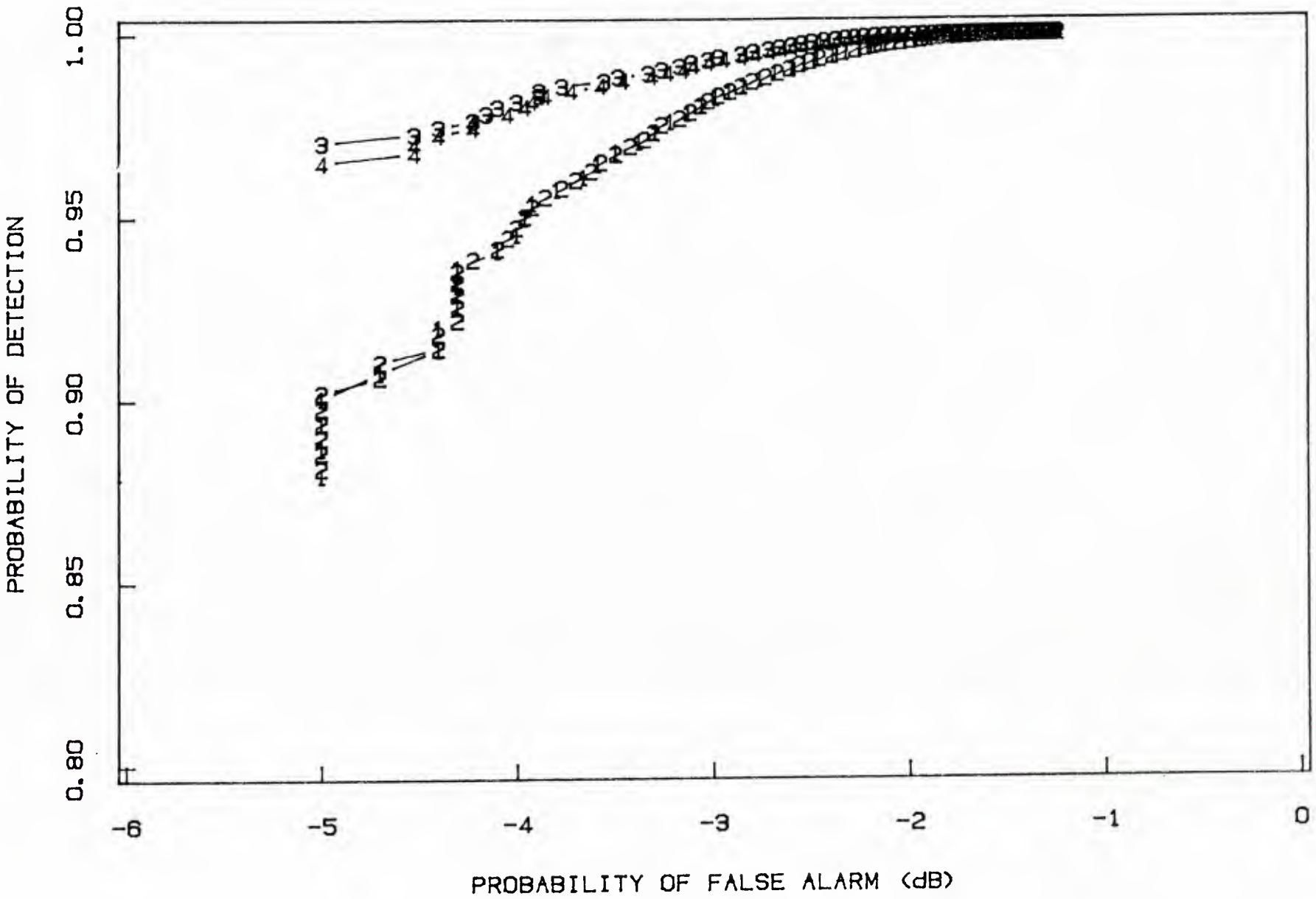


Figure 5.3
ROC curves for the MS noise and a pseudo-random signal

NON-LINEARITY ASSOCIATED WITH THE M. S. NOISE

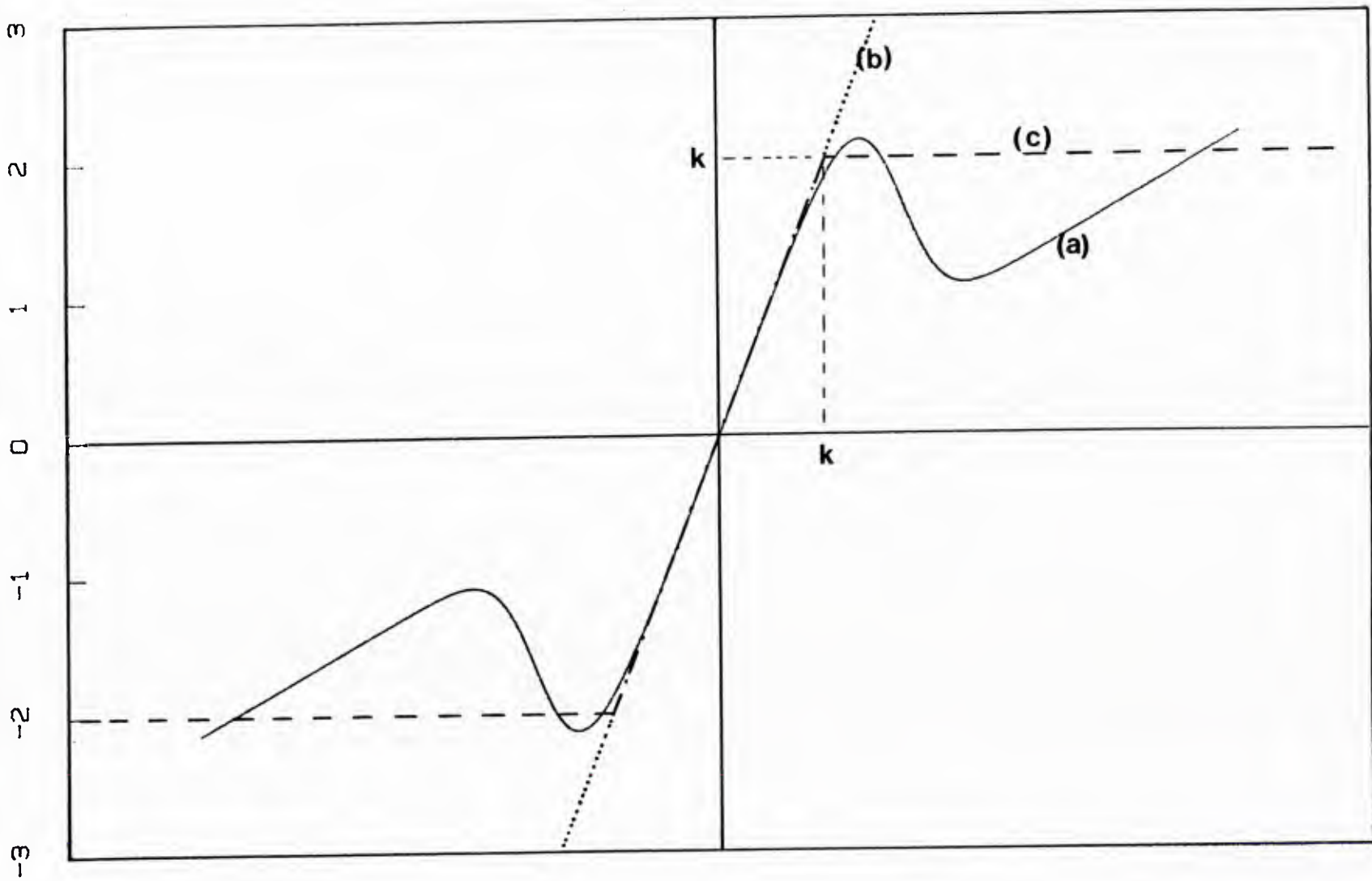


Figure 6.1

Test-function and non-linearities

- (a) mixture receiver
- (b) matched filter
- (c) soft-limiter

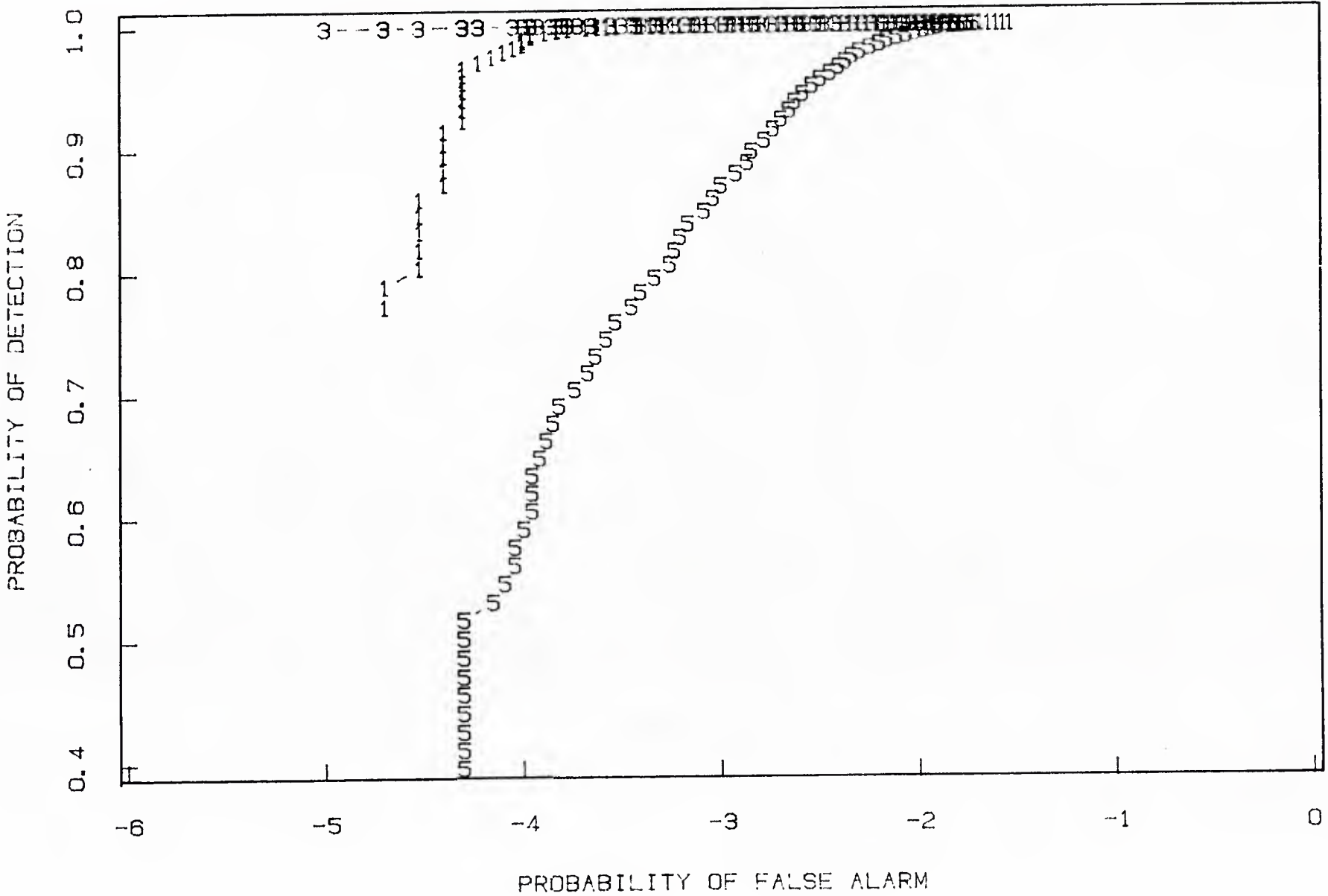


Figure 6.2
ROC curves for the MS noise and a constant signal
 $k = 1.4$, $SNR = 0$ dB

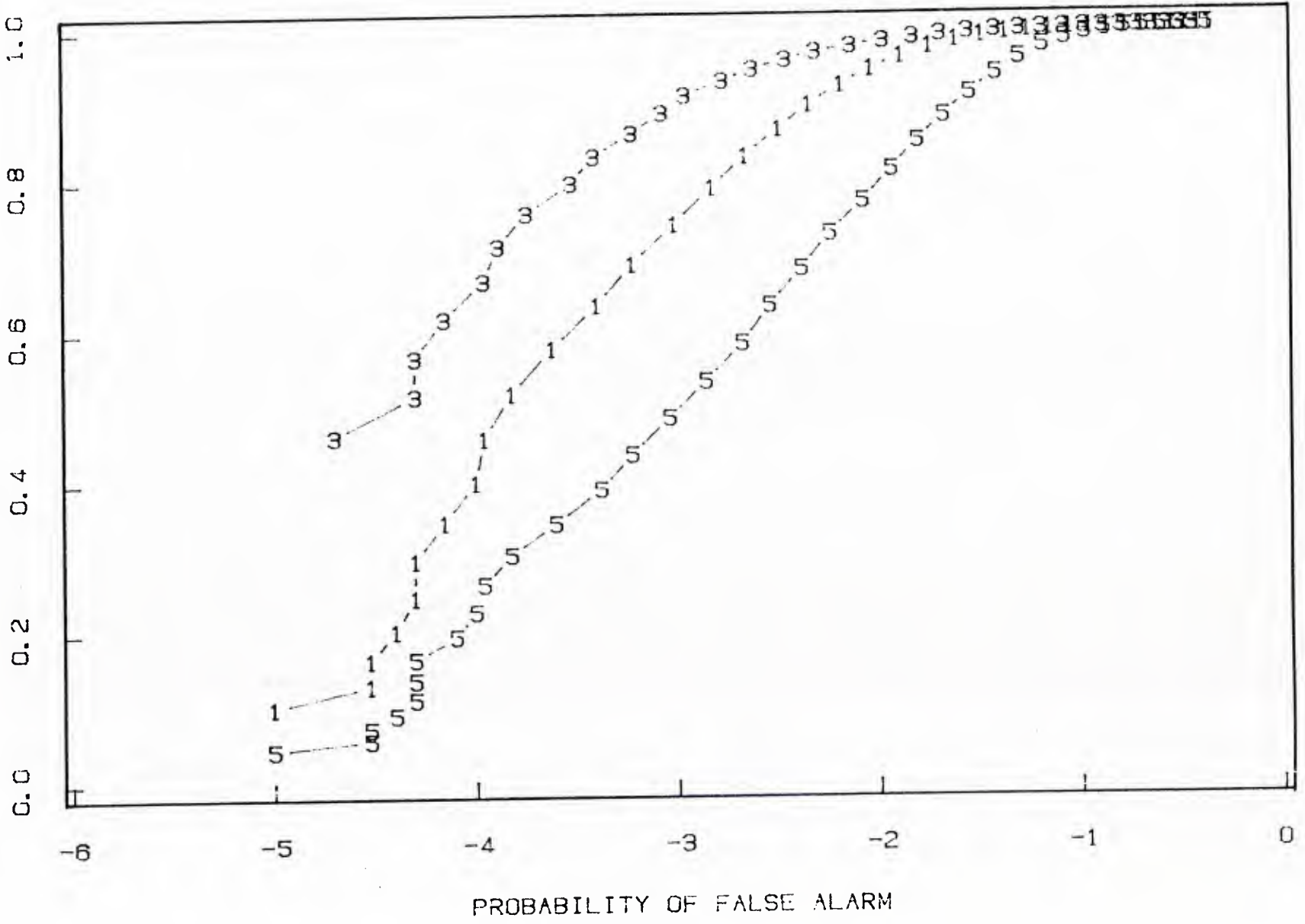


Figure 6.3
 ROC curves for the MS noise and a constant signal
 $k = 1.4$, $SNR = -5$ dB

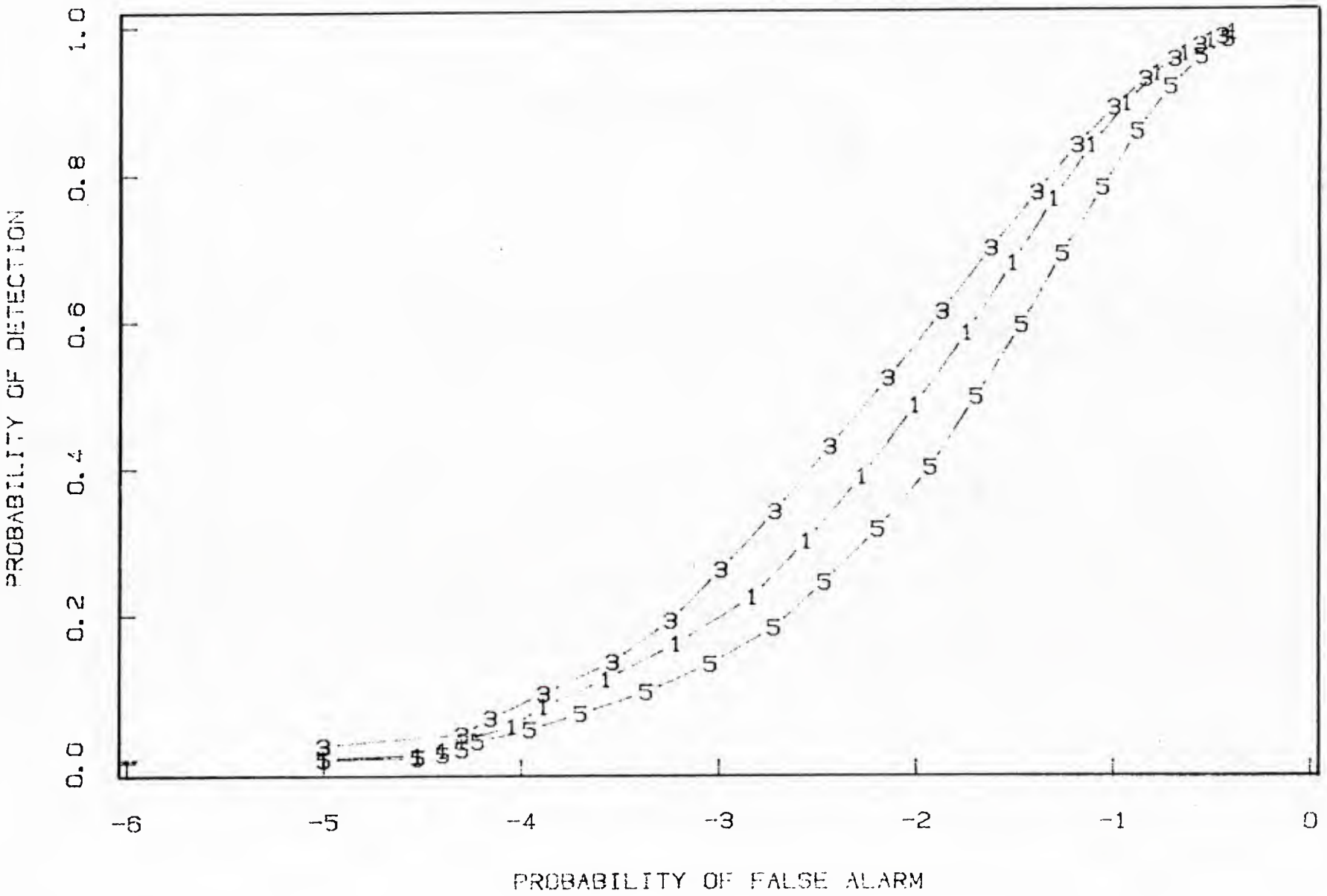


Figure 6.4
ROC curves for the MS noise and a constant signal
 $k = 1.4$, $SNR = -10$ dB

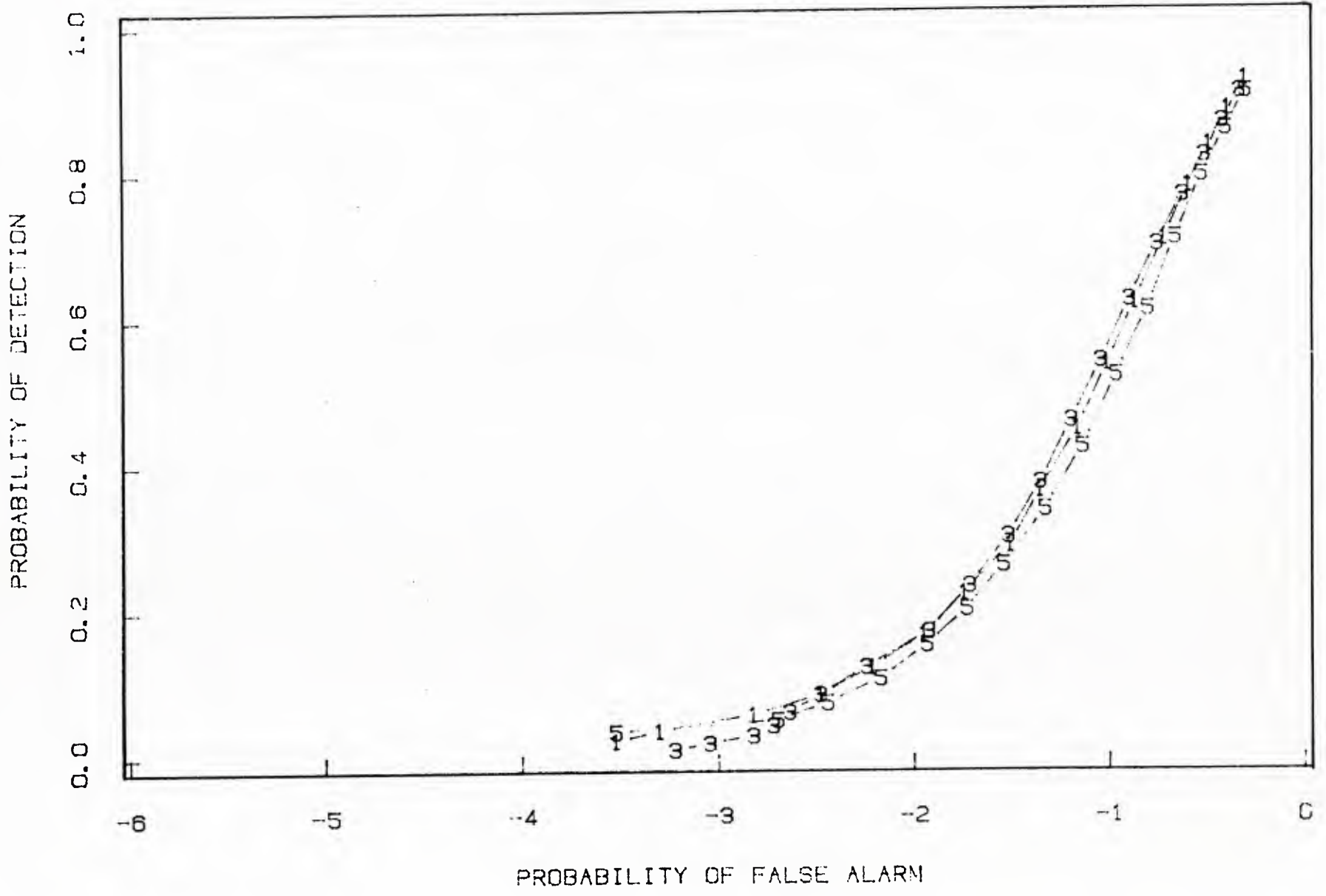


Figure 6.5
ROC curves for the MS noise and a constant signal
 $k = 1.4$, $SNR = -15$ dB

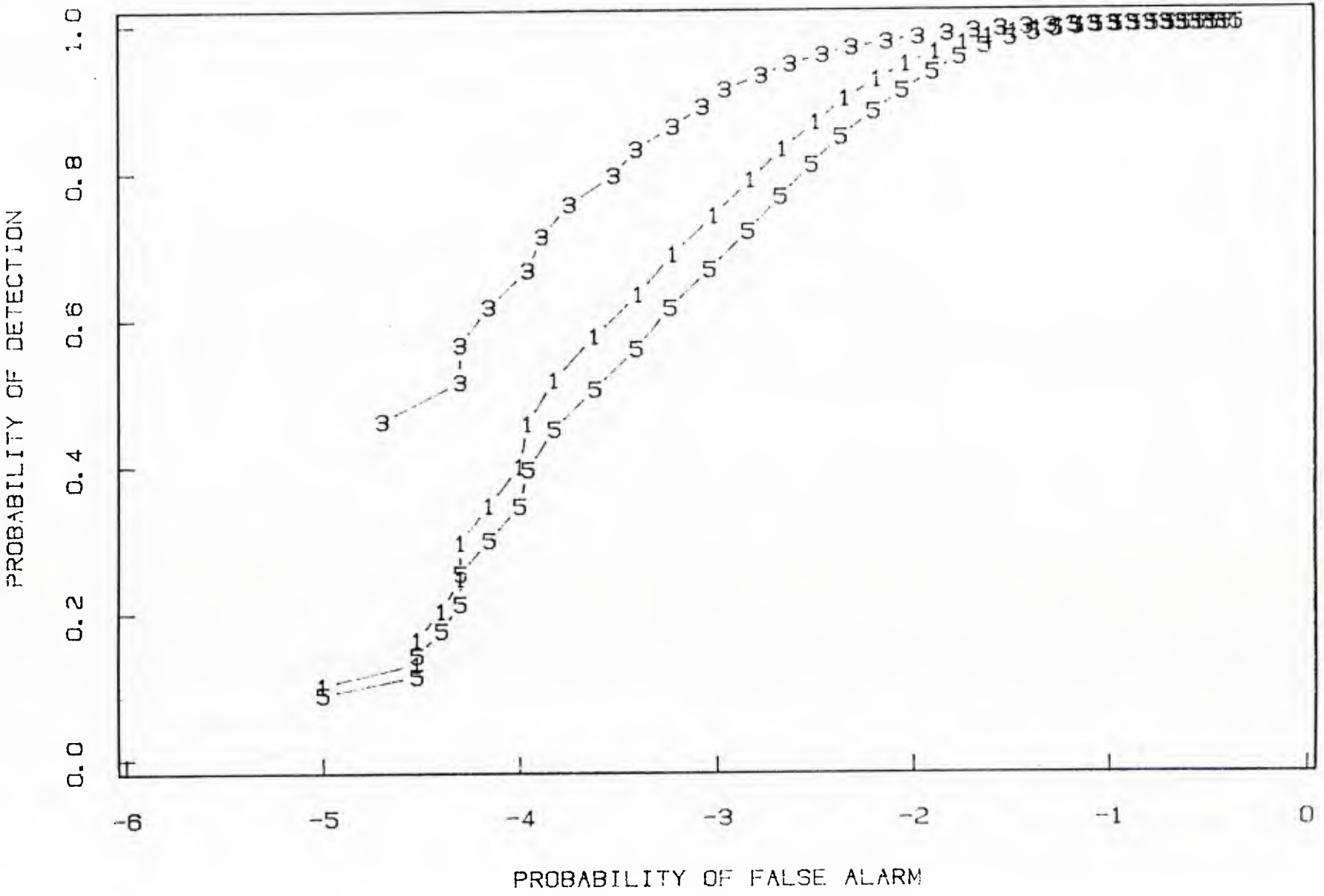


Figure 6.7
 ROC curves for the MS noise and a constant signal
 $k = 2.0$, $SNR = -5$ dB

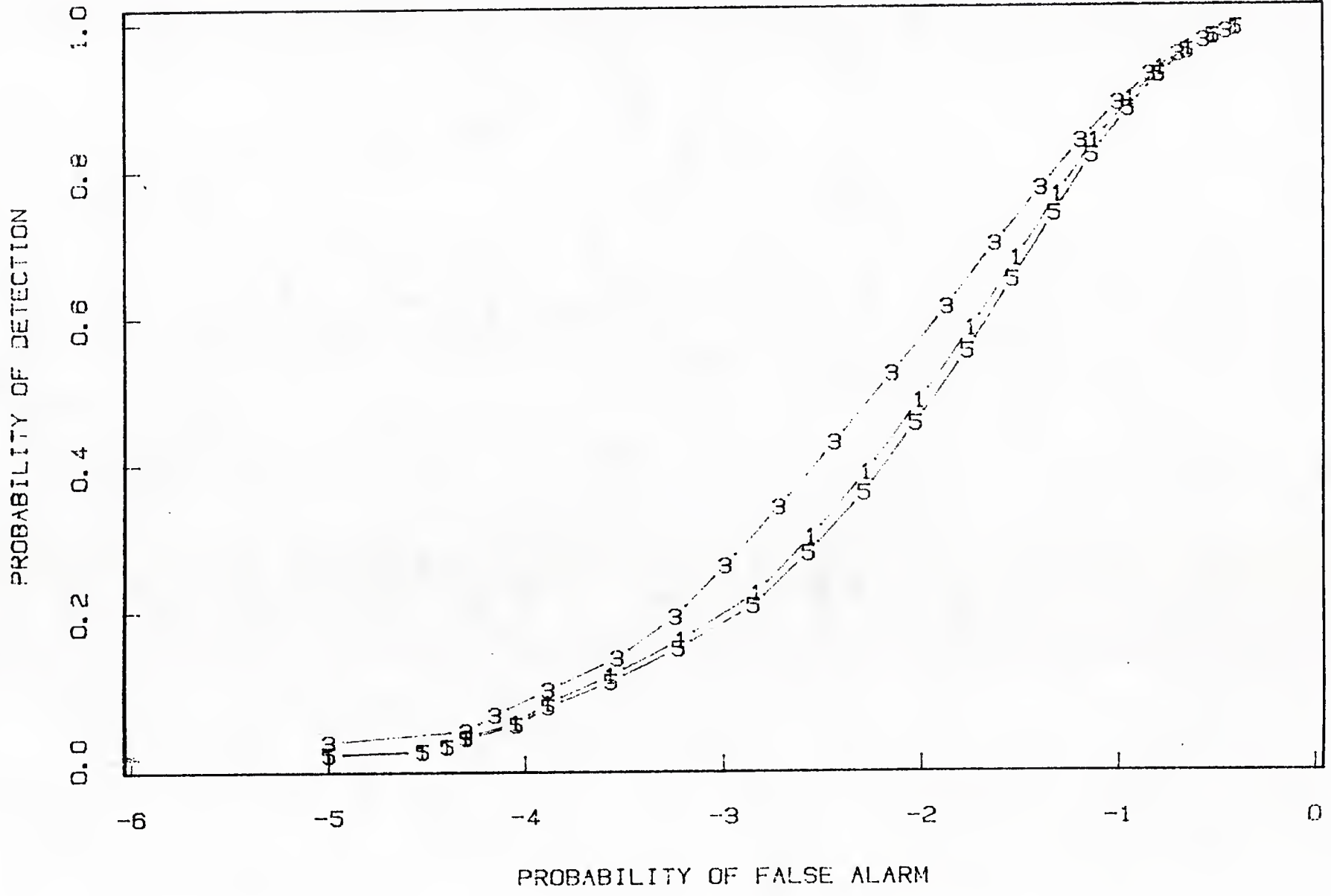


Figure 6.8
ROC curves for the MS noise and a constant signal
 $k = 2.0$, $SNR = -10$ dB

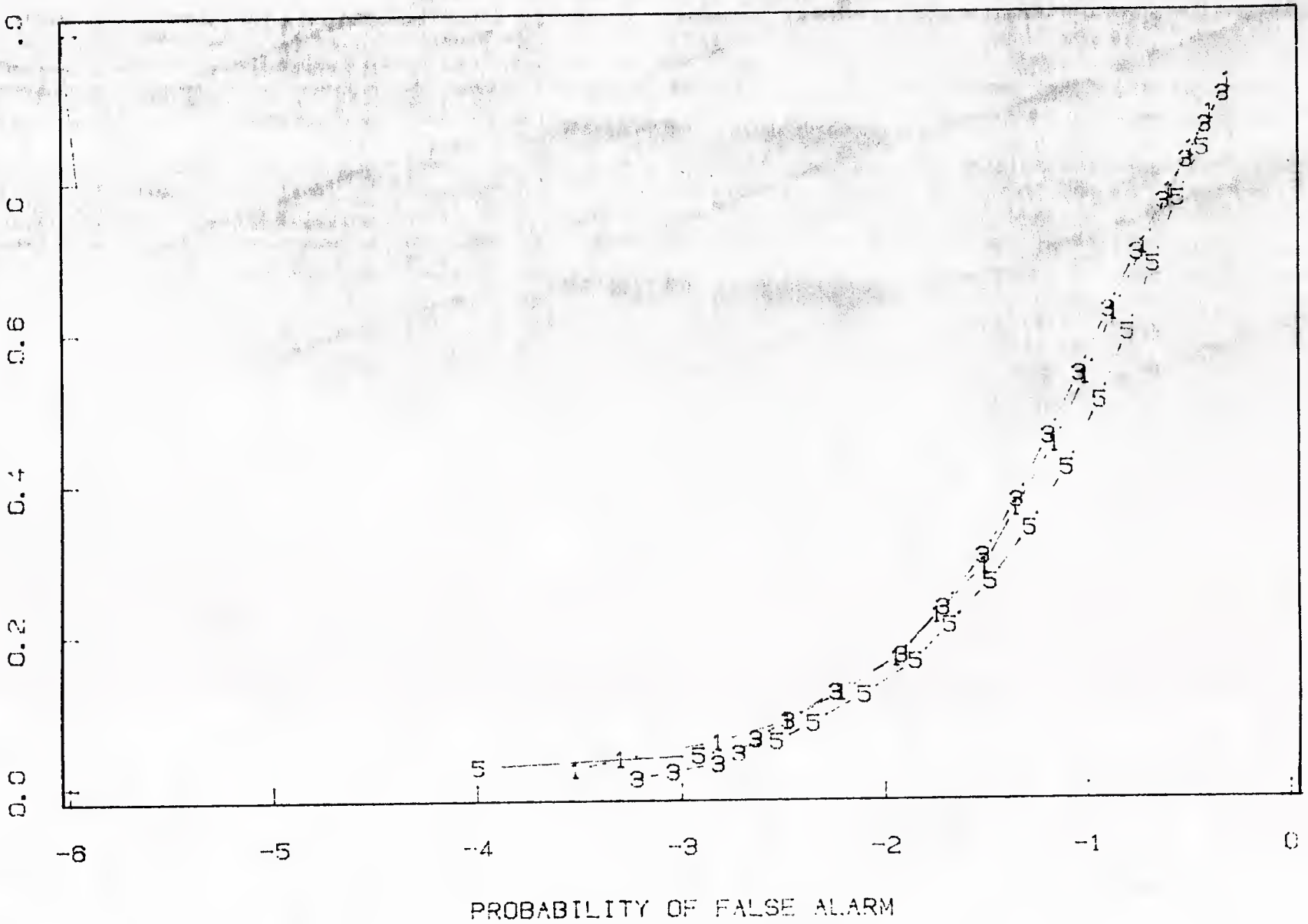


Figure 6.9
ROC curves for the MS noise and a constant signal
 $k = 2.0$, $SNR = -15$ dB

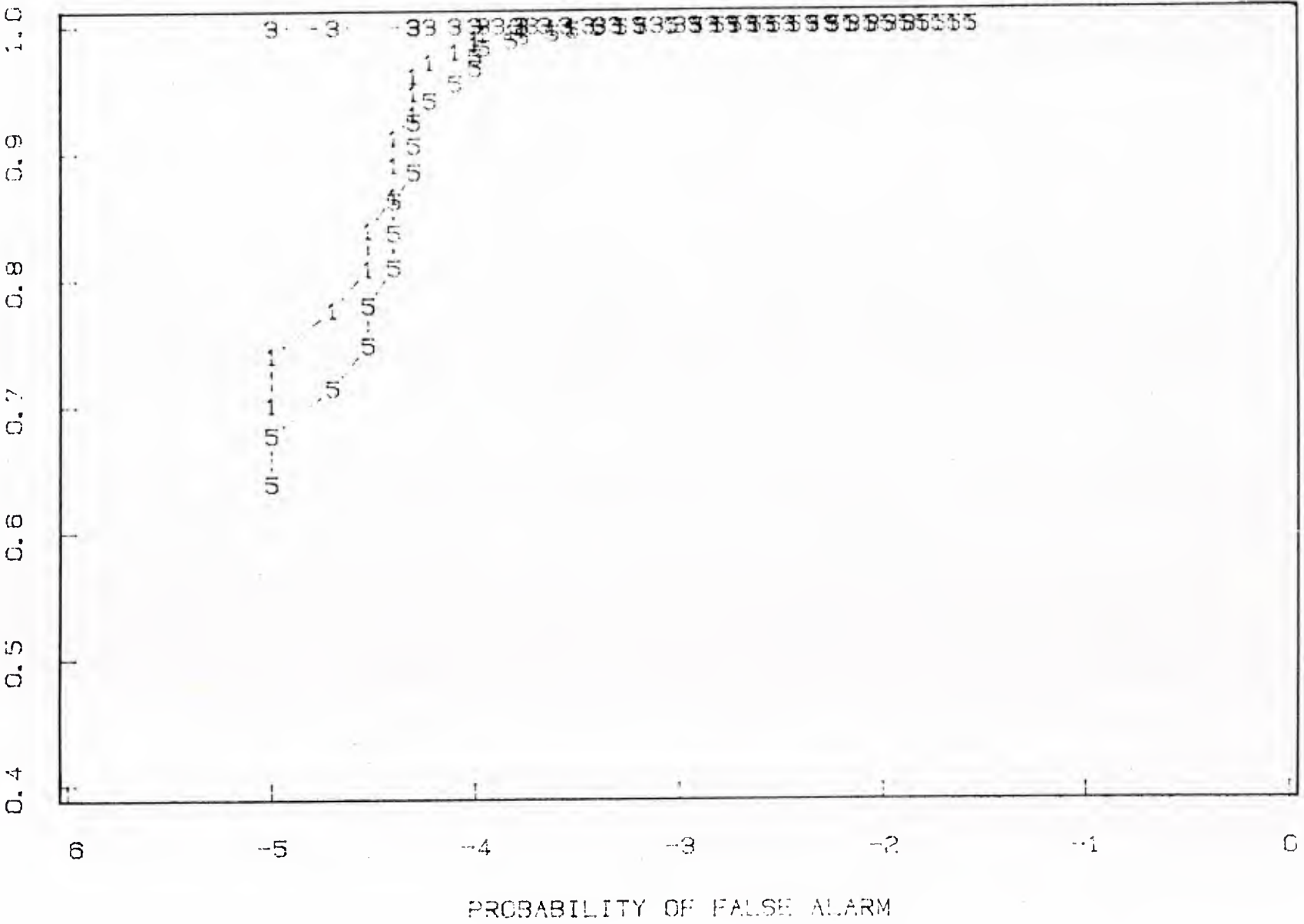


Figure 6.10

ROC curves for the MS noise and a constant signal
 $k = 2.5$, $SNR = 0$ dB

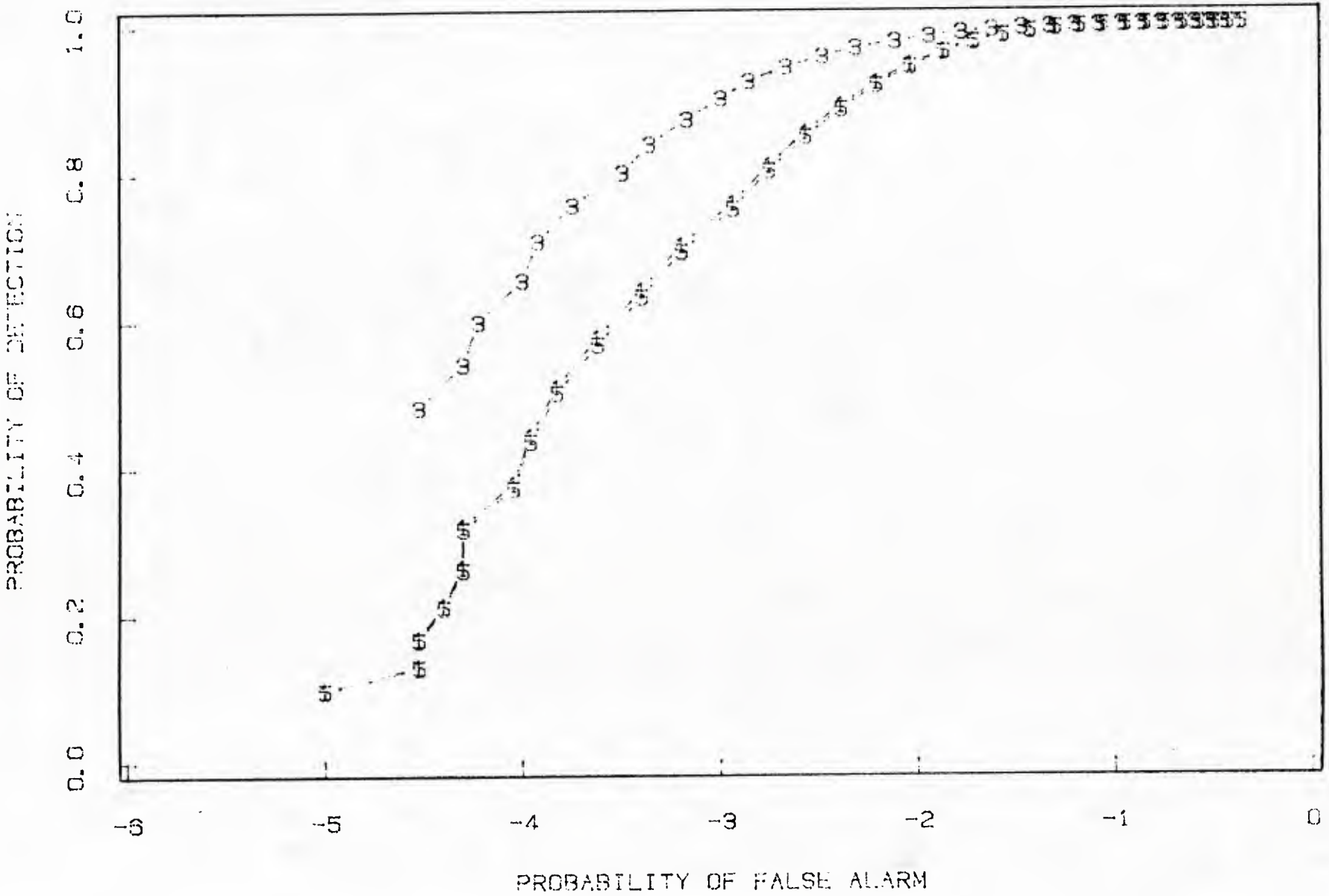


Figure 6.11

ROC curves for the MS noise and a constant signal
 $k = 2.5$, $SNR = -5$ dB

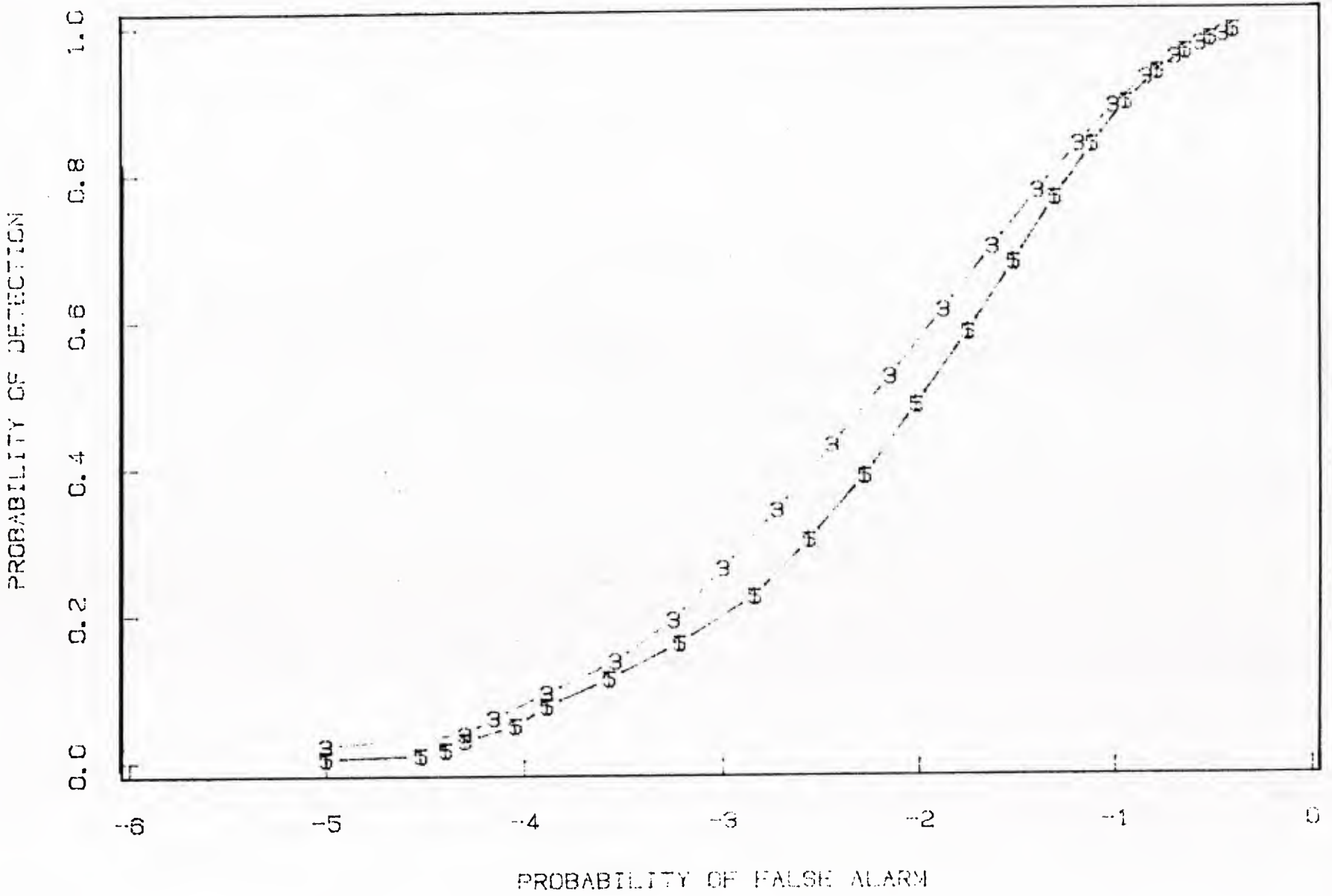


Figure 6.12
 ROC curves for the MS noise and a constant signal
 $k = 2.5$, $SNR = -10$ dB

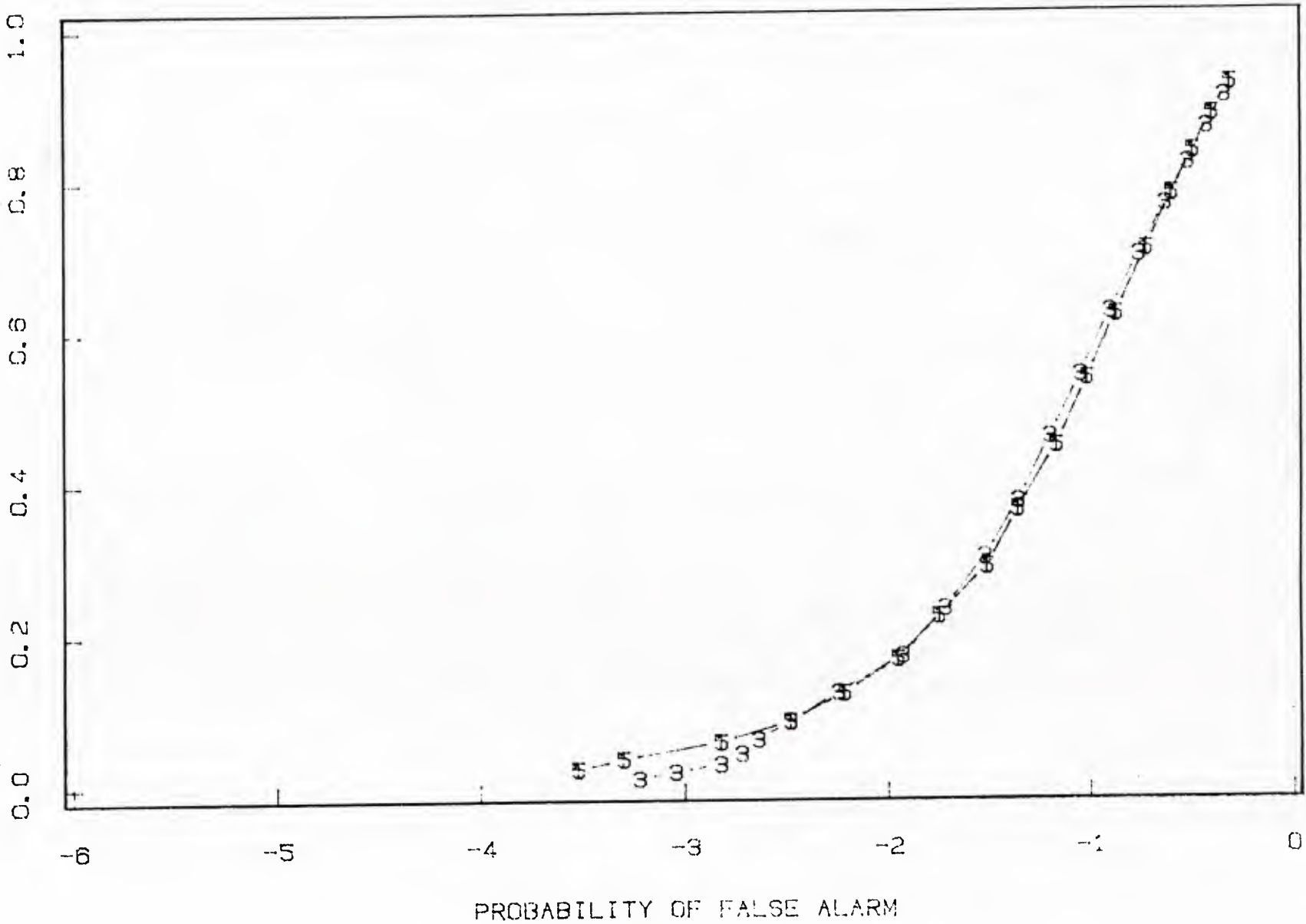


Figure 6.13
ROC curves for the MS noise and a constant signal
 $k = 2.5$, $SNR = -15$ dB

OFFICE OF NAVAL RESEARCH
STATISTICS AND PROBABILITY PROGRAM

BASIC DISTRIBUTION LIST
FOR
UNCLASSIFIED TECHNICAL REPORTS

FEBRUARY 1982

Copies	Copies
<p>Statistics and Probability Program (Code 411(SP)) Office of Naval Research Arlington, VA 22217 3</p>	<p>Navy Library National Space Technology Laboratory Attn: Navy Librarian Bay St. Louis, MS 39522 1</p>
<p>Defense Technical Information Center Cameron Station Alexandria, VA 22314 12</p>	<p>U. S. Army Research Office P.O. Box 12211 Attn: Dr. J. Chandra Research Triangle Park, NC 27706 1</p>
<p>Commanding Officer Office of Naval Research Eastern/Central Regional Office Attn: Director for Science Barnes Building 495 Summer Street Boston, MA 02210 1</p>	<p>Director National Security Agency Attn: R51, Dr. Maar Fort Meade, MD 20755 1</p>
<p>Commanding Officer Office of Naval Research Western Regional Office Attn: Dr. Richard Lau 1030 East Green Street Pasadena, CA 91101 1</p>	<p>ATAA-SL, Library U.S. Army TRADOC Systems Analysis Activity Department of the Army White Sands Missile Range, NM 88002 1</p>
<p>U. S. ONR Liaison Office - Far East Attn: Scientific Director APO San Francisco 96503 1</p>	<p>ARI Field Unit-USAREUR Attn: Library c/o ODCSPER HQ USAEREUR & 7th Army APO New York 09403 1</p>
<p>Applied Mathematics Laboratory David Taylor Naval Ship Research and Development Center Attn: Mr. G. H. Gleissner Bethesda, Maryland 20084 1</p>	<p>Library, Code 1424 Naval Postgraduate School Monterey, CA 93940 1</p>
<p>Commandant of the Marine Corps (Code AX) Attn: Dr. A. L. Slafkosky Scientific Advisor Washington, DC 20380 1</p>	<p>Technical Information Division Naval Research Laboratory Washington, DC 20375 1</p>
	<p>OASD (I&L), Pentagon Attn: Mr. Charles S. Smith Washington, DC 20301 1</p>

Copies

Copies

Director
AMSAA
Attn: DRXSY-MP, H. Cohen
Aberdeen Proving Ground, MD 1
21005

Dr. Gerhard Heiche
Naval Air Systems Command
(NAIR 03)
Jefferson Plaza No. 1
Arlington, VA 20360 1

Dr. Barbara Bailar
Associate Director, Statistical
Standards
Bureau of Census
Washington, DC 20233 1

Leon Slavin
Naval Sea Systems Command
(NSEA 05H)
Crystal Mall #4, Rm. 129
Washington, DC 20036 1

B. E. Clark
RR #2, Box 647-B
Graham, NC 27253 1

Naval Underwater Systems Center
Attn: Dr. Derrill J. Bordelon
Code 601
Newport, Rhode Island 02840 1

Naval Coastal Systems Center
Code 741
Attn: Mr. C. M. Bennett
Panama City, FL 32401 1

Naval Electronic Systems Command
(NELEX 612)
Attn: John Schuster
National Center No. 1
Arlington, VA 20360 1

Defense Logistics Studies
Information Exchange
Army Logistics Management Center
Attn: Mr. J. Dowling
Fort Lee, VA 23801 1

Reliability Analysis Center (RAC)
RADC/RBRAC
Attn: I. L. Krulac
Data Coordinator/
Government Programs
Griffiss AFB, New York 13441 1

Technical Library
Naval Ordnance Station
Indian Head, MD 20640 1

Library
Naval Ocean Systems Center
San Diego, CA 92152 1

Technical Library
Bureau of Naval Personnel
Department of the Navy
Washington, DC 20370 1

Mr. Dan Leonard
Code 8105
Naval Ocean Systems Center
San Diego, CA 92152 1

Dr. Alan F. Petty
Code 7930
Naval Research Laboratory
Washington, DC 20375 1

Dr. M. J. Fischer
Defense Communications Agency
Defense Communications Engineering
Center
1860 Wiehle Avenue
Reston, VA 22090 1

Mr. Jim Gates
Code 9211
Fleet Material Support Office
U. S. Navy Supply Center
Mechanicsburg, PA 17055 1

Mr. Ted Tupper
Code M-311C
Military Sealift Command
Department of the Navy
Washington, DC 20390 1

Copies

Copies

Mr. F. R. Del Priori
Code 224
Operational Test and Evaluation
Force (OPTEVFOR)
Norfolk, VA 23511

1